Addressing sperm DNA integrity and fertilization; establishment of a PCR based method for detection of DNA damage (the MDDA assay).

Jon Håvard Ryan

Master thesis in Toxicology

Department of Toxicology

Institute of Biology

UNIVERSITETET I OSLO

June 2011

Acknowledgements

The work related to this thesis was done at The Norwegian Institute of Public Health, under the Division of Environmental Medicine at the Department of Chemical Toxicology (MIKT). First, thanks must be given to my three supervisors at FHI, Ann-Karin Olsen, Hege Holte Slagsvold and Asgeir Brevik. Thank you so much for all the time, work and advice you have given me throughout these two years. The knowledge and patience who have given me will follow me forever.

Thank you also Nur Duale and Birgitte Lindeman for addition help, especially towards the end. Your advice was always thorough and accurate, and helped me greatly to reach my goals. I would also like to thank Heidi Plum Bjønnenes and Fredrik Fritzøe for addition help during these two years, both in the lab and for the friendships that developed.

Gunnar Brunborg, leader of MIKT, thank you for allowing me to work with you and your team. It has been a great experience for me.

I also wish to thank my supervisor from the University of Oslo, Steinar Øvrebø, for inspiring me to pursue further education in toxicology. Thank you for great lectures and your ability to teach.

To my friends and family, I never could have made it without the constant push from you guys.

Final thanks are given to my mum for all the help throughout this thesis, and my life, and to my girl, Si, for living with me throughout this master. Only a person with your patience could be capable of doing this.

Table of contents

Abstract

Humans in industrialized societies are continuously exposed to a plethora of environmental chemicals, of which the long-term consequences are largely unknown. Reduced fertility could be one such undesired consequence, and indeed reduced sperm quality is increasingly reported from many developed countries. Many environmental chemicals induce DNA damage, and sperm DNA damage is associated with reduced sperm quality, disturbed embryo development and early abortions. The present work was aimed at establishing a method to detect sperm DNA damage and to elucidate its impact on fertilization and early embryo development. Specifically we chose to study the widely distributed genotoxic benzo(a)pyrene (B(a)P) and glycidamide (GA; a metabolite of acrylamide), that most of us are exposed to on a daily basis. Determination of sperm DNA damage is a major challenge and at present there are no established protocols available. A less explored strategy is to assess DNA damage by the polymerase chain reaction (PCR). The easily accessible mitochondrial genome is more susceptible to DNA damage than the nuclear genome and thus represents a more sensitive target for the identification of sperm DNA damage. The PCR strategy involves a long amplicon (10 kb) for the determination of DNA damage relative to template number determined by a short fragment PCR assay (117 bp), the mitochondrial DNA damage assay (MDDA). The underlying concept is that DNA lesions will inhibit the DNA polymerase which is utilized in the long PCR assay to detect DNA damage: less PCR product equates to more DNA damage. The short PCR also reveals changes in mitochondrial genome numbers. The optimization of the method included determination of suitable DNA isolation and quantification procedures, along with appropriate PCR conditions, subsequently tested in cells exposed *in vitro* and frozen mouse tissue samples. Sperm and liver were harvested from mice exposed to B(a)P or GA a few days prior to sacrifice. The level of DNA damage in sperm and in liver was assessed by the MDDA. In parallel the sperm was used for *in vitro* fertilization experiments to determine fertilization rate and early embryo development. The MDDA proved successful in liver samples although more extensive optimization is required in sperm than was permitted within the scope of this MSc-thesis. Exposure to both B(a)P and GA gave rise to reduced fertilization rates with no indications of disturbance of early embryonal development at the doses used. In conclusion the MDDA is a promising tool for measuring DNA damage, and warrants further optimization for use in sperm. Moreover we verify that exposure to ubiquitous genotoxic agents influence fertilization.

Abbreviations

AA	Acrylamide
ATP	Adenosine triphosphate
B(a)P	Benzo(a)pyrene
Bp	Basepair
BPDE	Benzo(a)pyrene diolepoxide
BR	Broad range
BSA	Bovin serum albumin
Bw	Body weight
C1	Cell lysis buffer QIAGEN
CO_2	Carbon dioxide
Ct	Cycle threshold
CYP	Cytochrome P450
DNA	Deoxyribonucleic acid
ds-DNA	Double-stranded DNA
dH_2O	Distilled water
dNTP	Deoxyribonucleotide triphosphate
FCS	Fetal calf serum
G2	Digestion buffer QIAGEN
GA	Glycidamide
H_2O_2	Hydrogen peroxide
HCG	Human chorionic gonadotropin
HPLC	High-performance liquid chromatography
HS	High Sensitivity
HTF	Human Tubal Fluid
I.P.	Intraperitoneal injection
IUPAC	International Union of Pure and Applied Chemistry
IVF	*In vitro* fertilization
KSOM	K Simplex Optimization Medium
Log	Logarithmic
MDDA	Mitochondrial DNA Damage Assay
MEM	Minimum essential medium

MgOAc	Magnesium oxaloacetate
mRNA	messenger RNA
miRNA	micro RNA
MSc	Master of Science
mt-DNA	Mitochondrial deoxyribonucleic acid
NADP+/H	Nicotinamide adenine dinucleotide phosphate
nDNA	Nuclear deoxyribonucleic acid
PAH	Polycyclic aromatic hydrocarbon
PBS	Phosphate buffered saline
PCR	Polymerase chain reaction
PMSG	Pregnant Mare Serum Gonadotropin
Rpm	Revolutions per min
QBT	Equilibration buffer QIAGEN
QC	Wash buffer QIAGEN
QF	Elution buffer QIAGEN
QPCR	Quantitative polymerase chain reaction
RNA	Ribonucleic acid
ROS	Reactive oxygen species.
rRNA	Ribosomal ribonucleic acid
SD	Standard deviation
SMD	Sperm Mitochondrial DNA extraction
TAE	Tris-Acetate EDTA
Taq	**T**hermus **aq**uatis
tRNA	Transfer ribonucleic acid
UV	Ultraviolet

Introduction

1.1 General background

It can be argued that reproduction has always been the main goal from an evolutionary standpoint. Even though all living individuals are a product of a successful reproduction lineage, they themselves might not be as reproductively successful as their predecessors. Infertility is observed within both males and females of our species, and is defined by the American Society of Reproductive Medicine as the failure for a couple to conceive after one year of regular, unprotected intercourse (Honig *et al.*, 1994). It is estimated that 15 % of US couples will experience some form of infertility, of which 20% of these cases the male is the sole source to this (Hull *et al.*, 1985).

Human males contribute heavily to the germ line mutation load, being responsible for the vast majority of dominant genetic diseases passed on to offspring (Sawyer *et al.*, 2003). This is not always a negative function, as mutations drive the evolutionary process, and in the big picture are crucial for the survival of the species. Although, too many mutations are detrimental and can either have potential to reduce the quality of life, or challenge the continuation of the species. It is therefore important to understand the mechanisms for generating germ line mutations in males since they affect both the individual, as well as their offspring.

Throughout the previous decades, industrialized countries have observed several negative effects on the male reproductive system, primarily reduced sperm quality (Auger *et al.*, 1995; Carlsen *et al.*, 1992), but increasing incidences of testicular cancer, cryptorchidism, hypospadias and lower sperm count levels are also reported from many developed economies (Moline *et al.*, 2000). As a result of these conditions, artificial reproduction methods are highly desired.

Although many sophisticated tests are available, semen analysis is still the most important diagnostic tool used to assess male fertility, and includes parameters such as sperm count, motility and viability (Hwang *et al.*, 2011). A major shortcoming of semen analysis is that they do not capture DNA damage.

The sperm quality is of great importance for fertilization, and to the transfer of paternal genetic information to the embryo. Sperm DNA may be altered by either endogenous or environmental damage. An important form of endogenous damage is those that generate reactive oxygen species (ROS). Sperm is highly sensitive towards reactive oxygen species, although low levels of ROS are essential in preparing the sperm for fertilization, while higher levels may cause reduced mobility and DNA damage (Bansal and Bilaspuri 2010; Griveau and Le 1997). Furthermore it has been shown that paternal DNA-damages are transferred to the embryo (Sanova *et al.*, 2005).

1.1.1 Aims

The main vision was to establish a method to detect sperm DNA damage and understand its consequences for fertilization and early embryo development.

This thesis will focus on two environmental chemicals, Benzo(a)pyrene and Glycidamide (active metabolite of acrylamide). We aim will try to develop a method, based on the principles of the PCR, to detect DNA damage that is formed by these environmental chemicals.

By using this molecular biology technique, in collaboration with *in vitro* fertilization we will try to determine the level of damage these chemicals inflict on DNA, if any at all. We use a mouse model to mimic the reported low repair capacity observed in human testicular cells (Olsen *et al.*, 2003). The target tissue is sperm, although we use liver as a somatic equivalent. The liver is the first detoxification zone and where the greatest amount of damage is expected to be observed.

Aims

- Establish a PCR based method to detect DNA damage using the mitochondrial genome as proxy for nuclear DNA; the mitochondrial DNA damage assay (MDDA)
    1. Determine a suitable DNA isolation protocol
    2. Conduct accurate quantifications of low levels of DNA

3. Establish a short PCR method for accurate assessment of mitochondrial template concentration.
4. Establish a long PCR method to detect mitochondrial DNA damage.

- Verification of the working principle of the MDDA
  1. - In cultured cells exposed to genotoxic agents *in vitro*
  2. - In frozen liver tissue from mice exposed to genotoxic agents

- Investigation of mt-DNA damage in fresh liver and sperm in mice using the MDDA.

- To investigate implications of *in vivo* induced sperm DNA damage for *in vitro* fertilization and early embryo development.

1.2 Benzo(a)pyrene - a widely distributed environmental carcinogen.

Several chemicals have been linked to reduced fertility, notably solvents and heavy metals (Wellejus *et al.*, 2000). Evidence indicates that smoking and paternal exposure to pesticides are also associated with reduced fertility (Zenzes *et al.*, 1999). Cigarettes contain polycyclic aromatic hydrocarbons (PAHs) along with many other chemicals. One component of cigarette smoke is Benzo(a)pyrene (B(a)P), which is has often been regarded as the prototypical PAH.

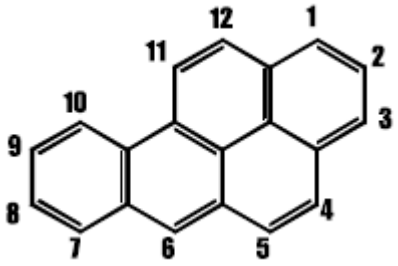

The structure of Benzo(a)pyrene, numbered by the IUPAC system.

B(a)P is a ubiquitous environmental pollutant produced during combustion processes. The story of B(a)P is long and notorious (Phillips 1983), first being noticed in the nineteenth century, when high incidences of skin cancer showed up amongst industrial workers. Many years passed with a large amount of scientific work being put forward, many suggesting the

negative side effects of B(a)P. It was not until the 1960s that Brookes and Lawley demonstrated the correlation between the carcinogenic potency of PAHs and their covalent bonds to DNA (Brookes and Lawley 1964).

Most human exposure to B(a)P is achieved via ingestion, inhalation or by dermal absorption (Kim *et al.*, 1998). It is estimated that 97 % of human exposure to B(a)P is due to ingestion (Hattemer-Frey and Travis 1991), although this is not the case for those who consume tobacco products or work within the coal industry, who will receive substantially higher intake from inhalation (Miller and Ramos 2001). B(a)P has been shown to induce bulky DNA adducts and is also capable of inducing oxidized base damage due to its ability to generate ROS (Briede *et al.*, 2004a; Olsen *et al.*, 2010). Due to the global build-up of work done and evidence presented on B(a)P, the chemical was upgraded from group 2B (possibly carcinogenic to humans) to group 1 (carcinogenic to humans) by the International Agency for Research on Cancer (IARC 2011), further emphasizing the risk and work that needs to be done within B(a)P.

1.2.1 Metabolism and toxicity of Benzo(a)pyrene.

Metabolism is the continuous breakdown and build-up of chemicals that occurs in cells. This ensures that the cell / organism degrades or receives the chemicals that it encounters, allowing it to grow, replicate or respond to its environment. B(a)P on its own does not pose any real threat to humans. It is due to our evolved metabolism that our own body releases the toxic and mutagenic potential of B(a)P. These metabolic enzymes are phase I and phase II enzymes, notably cytochrome P450 mixed function oxidases, epoxide hydrolases, epoxide reductases (phase I) and glutathione transferases, UDP-glucoronyl transferases and sulfotransferases (phase II) (Gelboin 1980).

B(a)P is metabolized to both water-soluble and organic solvent-soluble metabolites, predominantly to the (+)-enantiomer of anti-benzo(a)pyrene 7,8-diol 9,10-epoxide (BPDE). This product is from a two step reaction that first generates (-) B(a)P-7,8 dihydrodiol by the action of CYP1A1/CYP1A2 and CYP1B1, which is then further oxidized by the microsomal epoxide hydrolase to give BPDE, the suggested ultimate carcinogen of B(a)P, which is

involved with direct adduct formation (Alexandrov *et al.*, 2010; Shimada and Fujii-Kuriyama 2004; Sims *et al.*, 1974).

BPDE has been reported to be a very high inducer of tumors in the organs of mammalian species and has been shown to bind covalently to both deoxyadenosine and deoxyguanosine (Mensing *et al.*, 2005) via its epoxide ring at the 10 carbon position (Miller and Ramos2001). Guanine is especially targeted due to its low energetic properties. BPDE has been suggested to be a causative agent in various forms of cancer, mainly lung, endocrine, head-and-neck and female breast cancer (Shimada and Fujii-Kuriyama2004; Zheng *et al.*, 2010). Reports of atherosclerosis due to exposure to B(a)P from cigarette smoke have also been presented (Miller and Ramos2001).

BPDE is just one form of DNA adduct. B(a)P has the potential to generate a substantial amount of metabolites, many that can give rise to DNA damage in the form of lesions. The reason for this is that CYP-mediated B(a)P activation generates a range of metabolites, including phenols and arene oxides (Alexandrov *et al.*, 2010). Another example is the generation of dihydrodiols which may undergo $NADP^+$-dependent oxidation catalyzed by aldo-keto reductase (Akr superfamily) to yield the reactive and redox-active *o*-quinone (Benzo(a)pyrene-7,8-dione; BP-7,8-dione) (Penning 2004). The *o*-quinones can undergo two successive one-electron reduction reactions back to the catechol using NADPH cytochrome P450 reductases, or they might form oxidative DNA adducts. This is due to the redox cycle that generates ROS multiple times. Examples of ROS generated radicals are superoxide anion (O_2^-), hydroxyl radical (OH^-), and hydrogen peroxide (H_2O_2) (Penning2004).

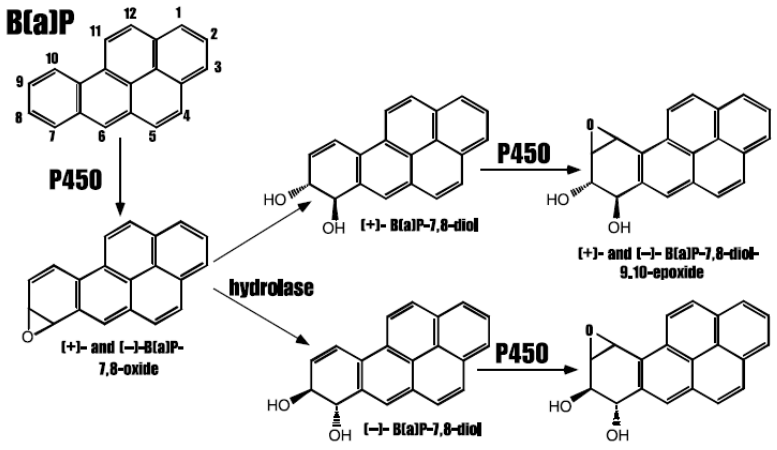

Transformation of B(a)P to its proposed ultimate carcinogen, BPDE (Shimada 2004).

1.3 Acrylamide (AA) and Glycidamide (GA) – environmental chemicals formed by processing of starches at high temperatures.

Acrylamide (AA) is an industrial chemical which is primarily used in the production of polyacrylamides, that can be used in water and petroleum purification (Segerback *et al.*, 1995). AA is also present in cigarettes, certain foods and drinks. AA is a water-soluble carbonyl compound that reacts with nucleophilic sites in Michael type additions (Segerback *et al.*, 1995). Formation of acrylamide is achieved during incomplete combustion or heating of organic matter, particularly glucose rich food such as French fries, potato chips, bread and biscuits (Tareke *et al.*, 2002). This formation is due to the Maillard reaction which generates acrylamide from reducing sugars and amino acids, mainly asparagine (Mottram *et al.*, 2002).

AA is known to produce a toxic response in many target organs, and cases of neurotoxicity, genotoxicity and carcinogenicity have been discovered (Segerback *et al.*, 1995). Within male reproduction toxicity, it has been shown that acrylamide has the ability to induce DNA damage in the male germ line (Bjorge *et al.*, 1996; Marchetti *et al.*, 1997; Sega *et al.*, 1990; Shelby *et al.*, 1986). This damage is in the form of DNA adducts, primarily with guanine, although all nucleic acid bases will react with AA, depending on energetic relations (Solomon *et al.*, 1985; V.Shelkovsky 2002). AA is metabolized both *in vitro* and *in vivo* to the epoxide glycidamide (GA) by the CYPE1 enzyme (Paulsson *et al.*, 2001; Settels *et al.*, 2008).

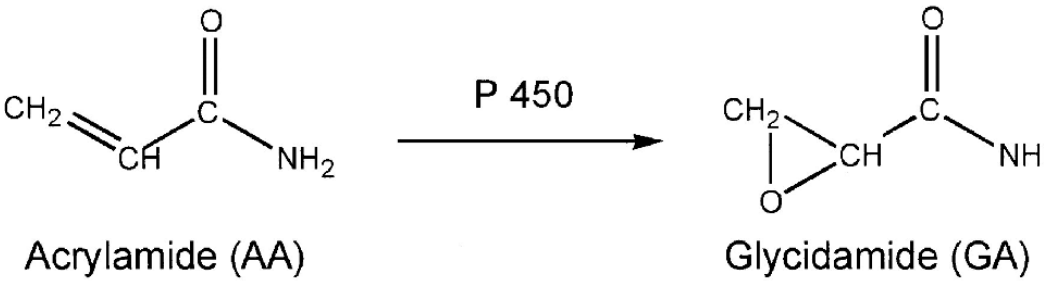

Transition from acrylamide to glycidamide, Paulsson 2001.

GA, in the same manner as AA, generates adducts with guanine at the N7 position (Calleman *et al.*, 1990). It has been proposed that GA is the ultimate carcinogen of AA (Generoso *et al.*, 1996; Settels *et al.*, 2008).

1.4 *In vitro* fertilization (IVF).

The history of IVF dates back to the late 1800s, where scientists were experimenting with the transfer of ovaries between animals of the same species (Fertaid 2011). Human experimentation on the other hand was difficult, therefore abandoned. It was not before the late 1960s that serious work was put into human experimentation. Although failure was common for the first decade, persistent work provided positive results (Wang and Sauer 2006). In 1978 the first successful human "test tube" baby was born, unleashing the public interest and potential uses of IVF (Steptoe and Edwards 1978).

Embryonic development in mammals is highly dependent on the biological processes that occur both before and after fertilization. The study of genes and pathways that are involved during these stages can give insight to how the organism matures and develops during the later periods of its life (Brison and Schultz 1997; Rodriguez-Zas *et al.*, 2008). In the initial phases after fertilization, all animal embryos utilize the genes and proteins present in the embryo, and rely strongly on these the first few days. The maternal genome is responsible for executing basic biosynthetic processes, directing the first mitotic divisions and specifying which regions of the embryo will differentiate to different cell types (Alberts *et al.*, 2002; Tadros and Lipshitz 2009).

The embryo then attempts to eliminate all maternal proteins and transcripts. This is initiated by maternal proteins that degrade the mRNAs. Zygotic transcription begins, producing proteins and micro-RNAs that degrade the remnants of the maternal mRNA and proteins (Tadros and Lipshitz2009). Among the first transcribed mRNAs are transcription activators, which enhance the genomic transcription. The zygote is now operating exclusively from the zygotic genome, which will sustain the organism for the rest of its life (Tadros and Lipshitz2009).

It is estimated that 15 700 genes are involved in the pre-implantation stage within rats (Stanton *et al.*, 2003). Reports have shown that paternal exposure to the anti cancer alkylating agent cyclophosphamide can alter expression of some of these genes, such as DNA repair genes (Harrouk *et al.*, 2000). It is proposed that genotoxic stress may disturb the nuclear remodelling and reprogramming events that follow fertilization and precede zygotic genome activation (Harrouk *et al.*, 2000). A relevant question is whether fertilization can be affected by introducing a more common and wide-spread environmental chemical, for instance B(a)P or GA to the paternal genome.

1.5 Target tissues - liver and sperm.

1.5.1 Liver

Due to its position between the intestinal tract and the rest of the body, the liver is the first organ where exogenous chemicals are metabolized and excreted. The liver will therefore have a higher toxic response to ingested chemicals compared to any other organ. This toxic response is determined by the exposure time and intensity, and can result in a plethora of injuries and diseases, for instance fatty liver, fibrosis, tumors and hepatocyte death (Curtis D.Klaassen 2008).

B(a)P has been shown to give bulky DNA adducts in liver and perhaps being the cause for elevated levels of ROS that were observed (Briede *et al.*, 2004b). It has also been demonstrated that the liver will receive higher levels of DNA damage than other organs, even if the other organs are exposed to higher levels of B(a)P (Park *et al.*, 2009).

1.5.2 Sperm

Sperm cells are produced in the testis and are responsible for transporting the paternal (haploid) genome to the oocyte during fertilization. Spermatogenesis is a complex development in which stem spermatogonia, through a process of mitosis, meiosis, and cellular differentiation, become mature spermatozoa (Ahmadi and Ng 1999). During this process, the sperm cell is sensitive to external stresses such as chemicals, radiation, toxicants and heat (Ahmadi and Ng1999).

DNA integrity in sperm is essential for the accurate transmission of genetic information and therefore the maintenance of good health in future generations. It has been shown that infertile men usually have large amounts of DNA damage within their sperm, reducing their quality and mobility (Ni *et al.*, 1997). Although, even with large amounts of damage, their ability to fertilize oocytes is still present, thereby transferring the genetic damage to the next generation (Ahmadi and Ng1999).

Recent studies of B(a)P exposure to mice have shown to increase the level of *de novo* mutations in spermatozoa, although bulky DNA adducts were not present (Olsen *et al.*, 2010). High amounts of chromosomal aberrations have been shown to be present in zygotes that have been fertilized by males exposed to acrylamide (Marchetti *et al.*, 1997).

1.6 DNA damage

DNA damage is a broad term describing anything that changes the genetic composition of the organisms original DNA, and can be divided into two classes, endogenous and environmental. The endogenous category includes mainly hydrolytic and oxidative reactions that are a consequence of cells being in contact with reactive oxygen (Friedberg *et al.*, 2006). The environmental category includes physical and chemical damage, which arise from outside the cell (Friedberg *et al.*, 2006). Examples of endogenous DNA damage are oxidation, hydrolysis and alkylation of bases and mismatch of bases due to errors in DNA replication.

DNA damage may either act on the sugar-phosphate backbone or on the bases themselves. Damage that affects the sugar-phosphate backbone may be in the form of low energy electrons, which have been shown to induce breakage on DNA strands (Zheng *et al.*, 2005). Damage may also be inflicted on the nucleobases, which often results in the covalent binding of metabolites to either one of the four (adenine, cytosine, guanine and thymine) (Curtis D.Klaassen2008). This type of damage is referred to as DNA adducts.

There are many examples of chemicals that promote oxidative damage to DNA, often being quite specific towards which base is targeted (Curtis D.Klaassen2008). These chemicals may result in either direct damage or indirect damage to DNA (Leadon *et al.*, 1988). During an

oxidative attack of DNA, guanine is often oxidised to 7,8-dihydro-8-oxoguanine (8-oxoG) (Gao *et al.*, 2004). 8-oxoG, which is the most frequent mutagenic lesion caused by oxidative stress (Larsen *et al.*, 2004), is a transformation caused by hydroxyl- radicals and superoxide radicals (Gao *et al.*, 2004) and occurs between 100-500 times per day per human cell (Lindahl 1993). This altered guanine base has a larger chance of base-pairing with adenine instead of cytosine, thus producing transversion errors after replication (Lindahl1993). Without repair mechanisms, such as DNA glycosylases, the cells life would quickly come to an end.

Another striking example of oxidative DNA damage, also caused by Benzo(a)pyrene, is the formation of thymine glycol. Thymine glycol has been shown to induce the same level of DNA damage as direct adduct formation. Since the formation of thymine glycol is just one of the many forms for indirect damage, this suggests that indirect damage is a larger contributor of DNA damage than direct damage (Leadon *et al.*, 1988).

Environmental damage is often due to exposure to ultraviolet (UV) light, heat, X-Rays or ionizing radiation (Brown 2006; Friedberg *et al.*, 2006). Ultraviolet radiation of wavelength 260 nm induces dimerization of adjacent pyrimidine bases, and will generate cyclobutyl dimers if two thymine bases are located next to each other (Brown2006). UV-induced damage causes deleterious mutations which will alter the DNA sequence after replication (Brown2006). Hydrolysis may induce the release of bases from their sugar component of DNA. This is accomplished when the β-N-glycosidic bond, usually on purines, is exposed to high temperature (Brown2006).

1.6.1 Mitochondrial DNA damage.

Mitochondria are membrane-enclosed organelles found in eukaryotic cells, most well known for their ability to generate adenosine triphosphate (ATP) and are therefore nicknamed the cells powerhouses (Henze and Martin 2003).

The mitochondrial genome is a haploid, circular molecule which is present in several copies, estimated between 2-10 (Wiesner *et al.*, 1992), in each mitochondrion. Depending on the cell type, anywhere between hundreds to thousands of mitochondria may be present in each cell. The human mitochondrial genome was sequenced in 1981 and concluded the size to be

16 569 bp (Anderson *et al.*, 1981). Although most of the mitochondria proteins (roughly 900) are encoded by the nuclear genome and later transferred to the mitochondria, the mitochondria still encodes 37 genes. Thirteen of these are protein subunits involved with cellular respiration, whilst 22 encode mitochondrial tRNAs and 2 encode rRNAs that work together in translation of mitochondrial transcripts (Chan 2006).

Exposure to genotoxic agents may result in the production and manifestation of DNA damage, mainly lesions or nicks in the genome. These lesions can lead to reduced transcription, cell cycle arrest or initiation of apoptosis (Ayala-Torres *et al.*, 2000). Evidence suggests that mitochondrial DNA is more susceptible to damage when compared to nuclear DNA (Richter *et al.*, 1988; Sawyer *et al.*, 2003; Yakes and Van 1997). This is mainly due to its positioning next to the electron transport chain (inner mitochondrial membrane), where ROS are frequently generated. This prompts an interesting "oxygen paradox", which is the fact that even though oxygen is an essential component in the formation of biological energy, it is extremely toxic to organisms due to the fact that DNA is highly susceptible to attack by ROS (Friedberg *et al.*, 2006).

Another reason that damage is so elevated in mt-DNA is the lack of the protective protein structures associated with nDNA (Santos *et al.*, 2006). Examples of DNA lesions that are not removed from the mt-DNA are: UV pyrimidine dimers (6-4 photoproducts), nitrogen mustard (complex alkylation) and N-nitroso-N-butylurea (O6-butyl-2'-deoxyguanosine) (Bohr 2002).

Early DNA extraction techniques, primarily phenol based, often induced more DNA oxidation damage than the samples actually contained (Helbock *et al.*, 1998). Other errors were due to handling errors done when mt-DNA was separated from nDNA (Anson *et al.*, 2000). Thus, more recent DNA extraction methods allow the isolation of mt-DNA without altering its genetic sequence.

1.7 The Polymerase Chain Reaction (PCR) and the influence of DNA lesions in the template.

The polymerase chain reaction, a simple and powerful method invented by K. Mullis and co-workers, allows amplification of DNA segments *in vitro* through a succession of incubation

steps at different temperatures (Mullis *et al.*, 1986). This reaction was made possible by the discovery and application of heat-stable DNA polymerases, most famously the Taq polymerase, initially isolated from the bacterium *Thermus aquaticus* (Chien et al., 1976). The reaction is typically as follows; the double-stranded DNA is heat denatured, and the two primers complementary to the 3' boundaries of the each strand and their target segment are annealed at low temperature and then extended at an intermediate temperature. This is referred to as a cycle. The PCR process is based on the repetition of this cycle, each time doubling the amount of PCR product, and can amplify DNA segments to great amounts with just 30 cycles.

A very useful feature of the PCR method is utilized in many different aspects of science. Originally designed to amplify small segments of DNA, it has now been converted to a much broader range of variations and applications, such as the hot-start PCR, reverse transcriptase PCR, multiplex PCR and ligation PCR (Birch 1996; Freeman *et al.*, 1999; Hayden *et al.*, 2008; Stemmer *et al.*, 1995).

Another such modification came in the early 1990s. Scientists who then were working on quantifying DNA damage desired a new method as the Southern Blot technique had to many limitations, mainly the large amount of DNA that was required, and the knowledge of restriction enzyme flanking sites of the sequence of interest. This resulted in the introduction and continual modification of the quantitative polymerase chain reaction (QPCR) (Kalinowski *et al.*, 1992). Since the reaction and results are produced "in real time", the method also goes under the name "Real-Time PCR".

QPCR is an innovative technique that allows quantification of nucleic acids with extreme accuracy during a PCR procedure (Higuchi *et al.*, 1993). Fluorescent reporters monitor the accumulation of double-stranded products with each successive cycle, constantly measuring the increase of fluorescence during the exponential phase against the background fluorescence. As the reaction reaches the first stages of significantly detectable exponential growth, the Ct (threshold cycle) value is determined and presented (Chen *et al.*, 2007), usually via computer software.

One of the many useful applications of conventional PCR is that it can be used as a measurement of DNA damage. This assay is based on the principle that several types of stable

DNA lesions will have a negative affect on the amplification of template DNA, either by haltering or stopping elongation completely (Ayala-Torres *et al.*, 2000; Ponti *et al.*, 1991). DNA lesions and enzyme blockage have also been demonstrated several times in the past, for instance it has been shown that digestion of DNA by lambda exonuclease is blocked by some types of DNA damage, particularly compounds that bind to the minor groove of DNA (Mattes 1990). Inhibition of *in vivo* replication has also been documented, due to lesions formed at the N7 positions of guanine (Pinto and Lippard 1985). Experiments can therefore be designed using different samples and exposure levels to determine the degree of damage within the genome, under the requirement that the starting number of DNA templates for all samples is equal. Testing has shown that biological samples exposed to ultraviolet (UV) light reduces PCR yields in comparison to control DNA (Van Houten B. *et al.*, 1998). Similar experiments have been done using chemical damage, in the form of H_2O_2, also resulting in lower yields (Ballinger *et al.*, 1999; Santos *et al.*, 2006).

The main difference between QPCR and conventional PCR is that in QPCR you monitor the progress of the PCR as it occurs. Data is collected throughout the PCR process rather than at the end of the process. In QPCR, reactions are characterized by the point in time during cycling when amplification of a target is first detected, rather than the amount of product accumulated at the end of PCR (Applied Biosystems 2011).

1.8 Quantifying DNA concentrations.

DNA has now become a household name known to many as being the blueprint of life. Science has long known the benefits of working with DNA, in everything from genetic research to use in crime scene investigations. DNA is found in all living organisms and is transcribed into RNA, which is later translated to proteins.

Friedrich Miescher, a young Swiss doctor, was the first person to discover and extract DNA from a living sample (Dahm 2010). This work was done between the years 1869 and 1870. He even speculated that DNA could be related to hereditary traits, although he later rejected his own idea (Dahm2010). Therefore, DNA was not thought to be the carrier of genetic information until the experiments of the mid 1940s by Avery and colleagues (Avery.O.T. *et al.*, 1944). In 1953, Watson and Crick suggested the structure of DNA (Watson and Crick

1953), which today is still accepted as accurate. Their double-helixed, molecular model of DNA was based on the work on X-Ray diffraction done by Rosalind Franklin and Raymond Gosling.

Many applications of science demand exact quantification of DNA, or else results may be misinterpreted. To attain numerical values, one must use spectrophotometry, which is the measurement of the reflection of transmission properties of a material as a function of wavelength (Allen 2010). We explore two different variants of this science, one relying completely on the principle of optical density, the Nanodrop 1000, and one using fluorescent dyes that bind to double-stranded DNA, the Qubit fluorometer. Emphasis was placed on accuracy, cost, and user friendliness.

2. Materials and methods

2.1 Mice and chemical exposures.

Male mice (strain B6D2F1 from Charles River Laboratories, 8-12 weeks of age) were exposed to either GA or B(a)P and each exposure group had its own separate control group. GA animals received one injection (61mg/kilo, i.p.) eight days prior to the experiment. The corresponding control group was injected with an equivalent volume of corn oil (i.p.). B(a)P animals received one injection (150 mg/kilo, i.p.) four days prior to the experiment and the corresponding control group was injected with an equivalent volume of phosphate buffered saline (PBS).

The mice were euthanized by either cervical dislocation or asphyxiation with CO_2.

Cauda was promptly removed and stored in eppendorf tubes containing 500 µl M2 medium. Liver samples from B(a)P experiments were also harvested and stored in 500 µl M2 medium and isolated following the QIAGEN Blood and Cell kit isolation procedure.

2.2 *In vitro* fertilization.

Females received an injection containing pregnant mare hormone gonodotropine (PMSG) three days prior to the IVF experiment. They received an additional injection, this time with human chorinic gonodotropin (HCG) one day before the IVF experiment. On the day of the IVF, the female mice were euthanized by either cervical dislocation or asphyxiation with CO_2. Oviducts were promptly collected, and stored temporarily in eppendorf tubes containing 500 µl M2 medium. Egg clutches, each including between 10-20 oocytes, were extracted from each oviduct. Eggs were then quickly transferred to a new dish, containing a droplet of 250 µl HTF, surrounded by liquid paraffin.

The cauda was transferred to a small dish containing 250 µl of HTF (surrounded by liquid paraffin). Small incisions, using micro scissors, were made to the cauda to release the sperm,

which were left for 10 min before the IVF was performed. Cauda sperm samples from B(a)P animals was collected and isolated via the Triton-X method.

1 ml of either control or exposed sperm was then transferred to the dish containing oocytes, which was then placed in the incubator at 37 °C with 5 % CO_2. To ensure that each female mouse was included in both the control and exposed samples, the left side oviducts were fertilized with exposed sperm, while the right side oviducts were fertilized with control sperm. These were left to fertilize for 4,5 hours.

After fertilization the embryos were washed 5 times in 250 µl KSOM, and then transferred to a new dish containing 250 µl KSOM, which also was surrounded by liquid paraffin. Photographs were taken at the different stages of embryonic development, notably fertilization, the first mitotic stages and cell death.
This was done by placing embryo dishes on the stage of a ZEISS AXIO, and by using the software program NIS Elements F.

2.2.1 Counting and collection of embryos, evaluation of fertilization index.

Each IVF experiment contained between 20-100 starting embryos. To determine if any differences between oocytes were present between those that have been fertilized with sperm from control or exposed animals, counting of embryos that pass on to the next mitotic stage was done.

2.3 Cell culture and experimentation.

2.3.1 Plating out cells.

We used the Hepa1c1c7 cell line (mouse hepatocyte cell line) for all experimentations involving cultured cells. These were stored in nitrogen tanks before use, and in 37 °C incubators with 5 % CO_2 when in use. All cells are nourished with MEM-α medium with 10 % FCS and 0,1 mg/mL gentamicin.

2.3.2 Thawing and growing of cells.

a) The cells were defrosted by placing them in a preheated water bath at 37 °C for 2-3 min.
b) The cell line and passage number were noted before spraying the tube with 70 % ethanol.
c) The cells were then transferred into a 15 ml falcon tube containing 13 ml preheated medium containing serum.
d) Cells were spun at 8 °C at 1000 rpm for 5 min.
e) The supernatant was removed and the pellet was resuspended in 2 ml medium containing serum.
f) The resuspended cells were transferred in a 25 cm² flask and stored in the incubator at 37 ºC.

The cells were allowed to grow for at least three to five days before passaging, as initial growth after defrosting is slow. Control checks were performed on the cells every day under a microscope. Cells should be attached to the bottom of the flask, round and plump or elongated in shape. The colour of the media should be pinkish orange. If any of the cells were detaching in large numbers, looked shrivelled or if any signs of contamination were present, the cells were discarded.

2.3.3 Passaging

The growth of cells in culture follows a recognizable pattern. A lag period after seeding is followed by exponential growth called the log phase. Cells should be passaged when they cover the plate where the cell density exceeds the capacity of the medium. Maintaining the log phase will maximize the amount of cells that can be used for experimentation.

Procedure:

a) Required amounts of trypsin, PBS and growth medium containing serum were preheated to 37 ºC and carefully transported to the sterile bench. At this point, cells were checked for signs of contamination or deterioration. If either was discovered, the flask was discarded.
b) The old medium was removed from the flasks using a pipette and a pipetboy.
c) Cells were than washed twice with 10 ml (25 cm² flask) / 30 ml (75 cm² flask) PBS without

Mg and Ca, in an attempt to remove FCS that would inhibit trypsin used to release cells in the next step of the process. PBS also helped to wash away damaged or dead cells.
d) 1.5 ml / 5 ml (25 cm² flask / 75 cm² flask) of trypsin was applied to the cells, and left the flask was left for approximately 1-2 min at 37 ºC. Tapping on the sides and bottom of the flask released the cells.
e) The trypsin was neutralized by applying (10 ml / 30 ml) of medium containing serum. The cells were homogenized and separated by up and down pipetting.
f) The cell suspension (1 ml / 3 ml) was transferred a 25 cm²/ 75 cm² flask, containing 9 ml / 27 ml of fresh medium. The date, cell line and dilution ratio was noted, and the cells were cultivated in the cell incubator at 37 ºC.

2.3.4 Exposure of Hepa1c1c7 to H_2O_2.

As a guideline to determine the effects of B(a)P on DNA with respect to the PCR assay, a preliminary run was done on H_2O_2 to determine the level of damage one could expect.

Procedure:

a) Required amounts of trypsin, PBS and growth medium containing serum were preheated to 37 ºC and carefully transported to the sterile bench, where all necessary equipment was present. At this point, cells were checked for signs of contamination or deterioration. If either was discovered, the flask was discarded.
b) Cells growing in 75 cm² flasks were washed twice with 30 ml PBS.
c) The cells were loosened from the flask by addition of 5 ml trypsin, and left to incubate for 1-2 min at 37 °C.
d) Hitting the bottom and sides of the flask released the cells, which were suspended in 30 ml of preheated medium (containing serum).
e) The cells were homogenized and separated by up and down pipetting. The cells were kept in motion while performing the next step.
f) Calculation of cell amount was done by taking a sample of 50 ul and placing it on to a Bürcker chamber and counting the cells observed. The cell concentration/ ml was calculated, and 10 million cells were plated on each 10 ml Petri dish.
g) The cells were left for 24 hours in the incubator at 37 °C.

h) Stock H_2O_2 (30%) was diluted to 1% with nuclease free water in to a 15 ml falcon tube.
i) The medium was removed from the cells, which were then washed twice with 3 ml preheated medium (without serum).
j) 3 ml of medium (containing serum), with the correct concentration of H_2O_2 was added and then placed in the incubator for 1 hour.
k) The cells were again washed twice with 3 ml cold PBS.
l) The cells were scraped loose into a 2 ml solution of cold PBS using a rubber policeman, and transferred to a centrifuge tube on ice.
m) The Petri dish was washed with 2 ml cold PBS, which was added to the centrifuge tube.
n) The cells were recovered by centrifuging at 1500 x g for 10 min at 4 °C.
o) After discarding the supernatant, the cells were resuspended in 3 ml cold PBS.

2.3.5 DNA isolation from Hepa1c1c7 cells.

There are many different ways of isolating DNA, each with their own benefits and disadvantages. We used the QIAGEN Blood and cell kit for isolation of tissue and cells from culture. The QIAGEN genomic DNA purification procedure is designed for direct isolation of DNA with an average size of 50-100 kb (QIAGEN 2001). It is assumed that mitochondrial DNA will follow in this isolation, as a carry over effect.

Using a column to separate DNA from the rest of the cell contents (proteins, RNA and low molecular weight impurities) is based on several steps. First a cell lysis stage, followed by digestion of proteins and RNA, several washes, then by anion exchange to separate DNA from other contaminants. This is also highly beneficial as no phenols or chloroform is used which can cause further oxidative damage. Isopropanol is used as the final step to concentrate and desalt the genomic DNA.

2.3.6 Recovering DNA from H_2O_2 exposed Hepa1c1c7 cells.

a) Buffers C1, G2, QBT, and QC were placed on ice while buffer QF was preheated to 50 °C.
b) 2 ml of cell suspension was added to 2 ml buffer C1 and 6 ml distilled water. Mixing was done by inverting the tube several times.

c) The lysed cells were centrifuged at 4 °C for 15 min at 1300 x g. The supernatant was promptly discarded.
d) 1 ml of buffer C1 and 3 ml of distilled water were added to the pelleted nuclei, which was resuspended by vortexing. Another round of centrifuging at 4 °C for 15 min at 1300 x g was executed, again discarding the supernatant.
e) 5 ml of buffer G2 was added, followed by a short vortex stage of 10-30 seconds at maximum speed.
f) 95 µl of proteinase K was added followed by incubation at 50 °C for 30-60 min.
g) A QIAGEN Genomic-tip 100/G was equilibrated with 4 ml of Buffer QBT, and allowed to pass through QIAGEN Genomic-tip by gravity flow.
h) The sample was briefly vortexed for 10 seconds at maximum speed and applied it to the equilibrated QIAGEN Genomic-tip, where it was allowed to pass through via gravity flow.
i) The QIAGEN Genomic-tip was washed twice with 7.5 ml buffer QC.
j) The genomic DNA was then eluted with 5 ml of preheated QF solution.
k) 3.5 ml of cold isopropanol was added to the eluted DNA and the tubes were inverted 10-20 times to precipitate the DNA.
l) The DNA pellet was transferred to a 1.5 ml sterile eppendorf tube using either a small spatula or a tip. The DNA was washed with 500 µl of 100% ethanol followed by 70 % ethanol, each time centrifuging at 13200 rpm at 4 °C for 2 min and discarding the supernatant by pipetting the ethanol with a standard tip. The DNA pellet was then thoroughly dried, and left dissolve in 500 µl of HPLC grade water / Chelex treated water added desferal (5 mM).
m) After vortexing for 5 seconds, the DNA was left to dissolve on a rotating table overnight protected from light.

2.4 Tissue experimentation.

2.4.1 Recovery of DNA from liver tissue.

This isolation was performed using QIAGEN Blood and cell kit.

Procedure:

a) Buffers C1, G2, QBT, and QC were placed on ice while buffer QF was preheated to 50 °C.

b) A solution for homogenising the tissue/cells was prepared by mixing the following into a 50 ml Falcon tube; 9.5 ml buffer G2, 47.5 µl of a 1M solution of Desferrioxamine , 30.6 µl of RNase A (100U) and 10 µl of RNase T_1 (10U).
c) The tissue (80 mg) was thoroughly homogenized mechanically in the solution by using two large Dounce homogenisators. First a round of 6 times with pestill B, followed by 8 times with pestill A. This was done to break cells, and sub cellular components.
d) The homogenate was transferred to the 50 ml polypropylene tube and added 500 µl Proteinase K (20 mg / ml).
e) This was left to incubate at 37 °C for 2 hours or until the solution appeared clear.
A QIAGEN Genomic-tip 100/G was equilibrated with 4 ml of Buffer QBT, which was allowed to pass through QIAGEN Genomic-tip by gravity flow.
f) The sample was briefly vortexed for 10 seconds at maximum speed and applied it to the equilibrated QIAGEN Genomic-tip, where it was allowed to pass through via gravity flow.
g) The QIAGEN Genomic-tip was washed twice with 7.5 ml buffer QC.
h) The genomic DNA was then eluted with 5 ml of preheated QF solution.
i) 3.5 ml of cold isopropanol was added to the eluted DNA and the tubes were inverted 10-20 times to precipitate the DNA.
j) The DNA pellet was transferred to a 1.5 ml sterile eppendorf tube using a small spatula or a tip. The DNA was washed with 500 µl of 100% ethanol followed by 70% ethanol, each time centrifuging at 13200 rpm at 4 °C for 2 min and discarding the supernatant by pipetting the ethanol with a standard tip. The DNA pellet was then thoroughly dried, and left dissolve in 500 µl of HPLC grade water / Chelex treated water added desferal (5 mM).
k) After vortexing for 5 seconds, the DNA was left to dissolve on a rotating table overnight protected from light.

2.4.2 Recovery and isolation of DNA from cauda sperm with Triton X-100 and Proteinase K.

This isolation technique was experimented with as we desired a quick and easy method to isolate cauda sperm mt-DNA. This is based on release of mitochondria by Triton X-100, which acts as a detergent and permeabilizes the sperm tail. A short digestion of proteins by proteinase K allows for some purification before further proteins and contamination is removed by ethanol precipitation of DNA.

a) A solution of 0.5 % Triton X dissolved in PBS was prepared.
b) The cauda sperm was squeezed out of the cauda (see cauda squeezing guide) into 500 µl Triton-X solution. After this was done, the cauda tissue was discarded and the 500 µl Triton-X solution containing sperm was transferred to a 1.5 ml sterile eppendorf tube.
d) This was left for 15 min at room temperature, with vigorous shaking of the eppendorf tube performed every third min.
e) The solution was filtered with gauze (50 mm) into a new 1.5 ml sterile eppendorf tube.
f) 100 µl of 20 mg/ml Proteinase K was added and left to incubate at 55 ºC for 20 min.
g) The DNA was washed with 500 µl of 100% ethanol followed by 70% ethanol, each time centrifuging at 13200 rpm at 4 °C for 2 min and discarding the supernatant by pipetting the ethanol with a standard tip. The DNA pellet was then thoroughly dried, and left dissolve in 500 µl of HPLC grade water / Chelex treated water added desferal (5 mM).
h) After vortexing for 5 seconds, the DNA was left to dissolve on a rotating table overnight protected from light.

2.5 Quantifying DNA.

2.5.1 Qubit fluorometer

One method to determine DNA concentrations was by using a Qubit fluorometer. Our final concentration was set at 5 ng / µl. Instead of attempting to reach this value in one dilution, several dilutions stages were set up to ensure that the final concentration was as close to the goal as possible. These intermediate stages were set at 50 ng / µl, 20 ng / µl and 10 ng / µl.
Procedure:

a) For each sample, 199 µl of Quant-iT ds-DNA buffer (either HS or BR) and 1 µl of the 200 X dye were mixed together in either a sterile 1.5 ml eppendorf tube or a sterile 15 ml falcon tube. The solution was briefly vortexed.
b) 190 µl of this solution to was added to two Quant-iT tubes. 10 µl of provided ladder 1 was pipetted in to the first tube and 10 µl of provided ladder 2 was pipetted to the second tube. These ladders were than briefly vortexed and allowed to rest for 10 seconds before being measured in Quant-iT machine.

c) After the ladders had been successfully measured, 190 µl of buffer /dye solution was added to a new Quant-iT tube. 10 µl of the sample DNA was added and briefly vortexed. The sample was also allowed to rest for 10 seconds before being measuring. At least two duplicates were measured per sample.
d) The sample concentration was noted, calculated down to the next dilution stage and diluted. A new round of measurements was done to confirm that the sample had reached the new dilution stage.

2.5.2 Nanodrop-1000

Another established method for calculating DNA concentration was by use of the Nanodrop 1000. Before starting the measurements, the machine must be cleaned with nuclease free H_2O. The software program NanoDrop ND-1000 version 3.7.1 was opened and by choosing the "Nucleic acid" section DNA samples can be measured. A 2 µl blank must also be loaded and read by the machine to ensure that results are as accurate as possible. By applying and reading samples one can visualize peaks at different wavelengths and therefore estimate the purity of the DNA sample.

Procedure:

a) The software program (ND_1000) must be opened and the Nucleic Acid setting must be chosen.
b) A 2 µl sample was loaded onto the designated area and read by the machine, which generates a graph and a concentration value.
c) At least 2 duplicates were read per sample.

It is important that all results are checked for contamination by checking the ratio between the absorbance at 260 nm and 280 nm. Manuals suggest that ratio be roughly 1.8-2.0. Values outside this range indicate the presence of proteins or phenols.

2.6 PCR based methods for detecting DNA damage.

2.6.1 The long PCR assay, with mitochondrial genome as template.

The generation of DNA adducts plays a fundamental role in chemically-induced mutagenesis and carcinogenesis. The ability to detect these adducts is important in risk assessment of various exogenous and endogenous chemicals (Laws *et al.*, 2001). As previously mentioned, DNA adducts do frequently hinder the progression of DNA polymerases and can therefore be used to calculate the rate of DNA adducts that are present in the starting template.

As stated earlier, mitochondrial DNA is more exposed to damages inflicted by ROS, and is therefore a good candidate for studying effects of exogenous chemicals and their impacts on DNA with adduct formation as a primary issue.

The use of longer fragments (XL-PCR) improves the sensitivity of the assay by increasing the probability that adduct formation will occur. Therefore, use of a 10 kb mitochondrial fragment, which we are confident is large enough to receive at least 1 "hit" (DNA adduct formation), was chosen. Another reason for choosing the 10 kb fragment is that it reflects over 50% of the total nucleotide sequence of the mitochondria, thus giving a good chance of not being bias to certain areas of the mitochondrial genome. Previous work done by other groups have confirmed that the 10 kb fragment is large enough to receive between 0,4-2,5 hits when treated with H_2O_2 (Santos *et al.*, 2006).

Correct primer selection is crucial, and should in general consist of at least 20 bases with a G+C content of approximately 50 % and a annealing temperature close to 68 ºC (Santos *et al.*, 2006).

The primers for the 10 kb fragment are as follows:

5'-GCC AGC CTG ACC CAT AGC CAT ATT AT-3'	Sense
5'-GAG AGA TTT TAT GGG TGT ATT GCG G-3'	Antisense

The decision to use the GeneAmp XL PCR kit, which includes the rTth DNA polymerase, is based on previous work (Santos *et al.*, 2006). This polymerase is designed to amplify target

DNA sequences ranging from 5 to 40 kb in length when used in collaboration with the rest of the kit. The rTth DNA polymerase is also equipped with the ability to correct copy errors that often occur during PCR, thereby enhancing the reaction efficiency (Applied Biosystems 2006).

Generation of large fragments are dependant on several variables, mainly the extension time, pH, salt concentration, enzyme concentration and primer selection (Applied Biosystems2006). The PCR mixes were set up in two separate UV-hoods (one for preparation of the mastermix and one for preparation of DNA samples) to prevent any carryover DNA contamination.

Mix 1:

3,3 XL Buffer II:	15,15 µl
dNTP:	4 µl
10 kb Forward Primer:	2 µl
10 kb Reverse Primer:	2 µl
MgOAc:	2 µl
dH_2O:	9,85 µl
BSA (300 ng / µl):	20 µl
Totalt:	55 µl

Mix 2:

dH_2O:	4,5 µl
Polymerase:	0,5 µl
Total:	5,0 µl

Add the mixes (40 µl *mix 1*, 5 µl *mix 2* and 5 µl DNA sample) together in a small PCR tube and immediately run them with this program:

1) 94 ºC, 1 min.
2) 94 ºC, 15 seconds
3) 64.0 ºC, 10 min.
4) Step 2, rep 16.
5) 94 ºC, 15 seconds.
6) 68.0 ºC, 10 min.
7) Step 5, rep 4.
8) 72 ºC, 10 min.
9) Hold 4 ºC.

2.6.2 Setting up the short PCR (Real-Time PCR).

The short PCR procedure was done to compare potential loss of mitochondria throughout different samples. The decision to use the 117 bp primers is based on the assumption that the fragment is small enough to avoid receiving "hits" of any kind, thereby acting as a marker of how much starting template mitochondrial DNA is present. Differences in Ct values between samples that have the same starting DNA concentration of 5 ng / µl suggest differences in mitochondria amounts in starting sample.

The primers for the 117 bp fragment are as follows:

5'-CCC AGC TAC TAC CAT CAT TCA AGT -3'	Sense
5'-GAT GGT TTG GGA GAT TGG TTG ATG-3'	Antisense

The Real-Time machine and computer program that was used were both created by The Applied Biosystems, in our case we used the 7500 Fast Real-Time PCR System. This uses fluorescent based PCR chemistries to provide quantitative detection of nucleic acid sequences using end point and dissociation-curve analysis (Applied Biosystems2011). Advantages of the program are that it allows one to perform several assay types using the 96-well format, measuring each well independently, thereby allowing comparison of several samples simultaneously.

Protocol:

- The UV-light was turned on in both hoods for 30 min to destroy all DNA that might present.
- Work was started in the DNA-free hood, first mixing 10 µl mastermix + 1 µl of each primer (5 µM, resolved in nuclease free H_2O) per sample.
- The mastermix was then moved to the DNA hood, and the DNA samples were collected from storage.
-12 µl of mastermix and 10 µl of 1:10 DNA (0,5 ng / µl) were added to each well
- The plate was sealed with a lid and placed in the QPCR machine.

Although specific profiles for primers / controls could be programmed and selected, for instance the 117 bp reaction, every run had to be programmed manually. The program is listed as follows:

Stage 1	Step 1	95 °C 6 min	
Stage 2	Step 1	95 °C 15 seconds	Number of cycles: 40
	Step 2	60 °C 1 min	
	Step 3	72 °C 35 seconds	
Stage 3	Step 1	95 °C 15 seconds	Dissociation stage
	Step 2	60 °C 30 seconds	
	Step 3	95 °C 15 seconds	

Data collection: stage 2, step 3
Volume in wells: 22 µl

2.7 Processing of results from long and short PCR experiments.

2.7.1 Preparation of agarose gel for long PCR products.

The PCR products were run on a 0.7% agarose gel. This gel consists of 3.5 g agarose and 500 ml 1X TAE buffer which were mixed together in a 600 ml glass beaker. This was then heated at maximum temperature in a microwave for 5-6 min until all the agarose had been dissolved. Cooling with cold water and constant stirring prevented the gel from solidifying before being

cast in the mould. When the gel reached a temperature of approximately 50 °C, 20 µl ethidium bromide was added at the gel poured into the mould and left to solidify.

The gel chamber was filled with approximately 800 ml 1X TAE buffer before adding the solidified gel. 20 µl of PCR product was mixed with 4 µl 6X gel loading dye in a small PCR tube, before applying 20 µl of this mixture to the gel. 10 µl of ZipRuler ladder was also loaded to a separate well. (see Appendix A for ladder definitions).

For best separation, the gel was run for 15-20 hours at 30V.

2.7.2 Quantification by densitometry.

Once the gel had run and was removed from the chamber, it was placed in a Kodak Gel Logic 2200 Imaging System to be taken a photo of. Using the software program Molecular Imaging, also by Kodak, it was possible to determine the fragment sizes and weights (after programming in the ladders). Exposure time was set at 4 seconds and number of exposures was set to at least 10 to ensure good pictures of each photo.

2.7.3 Long PCR results.

2-6 duplicates of a single DNA sample were amplified by the long PCR assay. These samples were then loaded onto a gel, run overnight and then photographed. Their gel band values from were added together and their mean value was calculated, along with their standard deviation. Samples were converted to percent values, where the control was always set at 100 %.

Loss of mitochondria that was shown via QPCR was calculated and used to adjust the values, giving a final difference between exposed and control samples. Differences between exposed and control samples were also converted to lesions per fragment size (10 kb) by using the equation L = -ln(Exposed-Control) (Santos *et al.*, 2006). This is based the Poisson distribution that requires the assumption that DNA lesions are randomly distributed.

2.7.4 Evaluation and correction of mitochondrial loss.

Ct values from exposed DNA and control DNA were collected after each successful QPCR. Each QPCR sample had between 4-10 duplicates. Mean values were calculated and standard deviation was noted. These values were converted to linear numbers (2^Ct) and compared against one and other and to decide if any difference was present. If a difference was observed, this difference was used to adjust the results of the long PCR.

Short PCR products were periodically run on either a 2.2 % FlashGel to ensure that no unspecific binding of the primers had occurred (see Appendix A for ladder definitions).

2.8 Statistical analysis.

Results are presented as the mean ± SD. Generally Student's t-tests for independent samples were used to test for differences before and after treatment in values that had been log-transformed and long PCR data from densitometric analysis of gel photos. Spearman correlations were uses to determine associations between dilutions and PCR amplification in efficiency plots. Chi square tests for independence were used to test differences in survival between embryos of exposed fathers and control embryos. Mean values were considered to be significantly different from each other when $P < 0.05$. Instances where drastically lower P values are observed are shown to emphasize the significance of the results.

3. Results

3.1 The establishment of a short PCR and a long PCR assay for detecting DNA damage; the mitochondrial DNA damage assay.

The main aim of this work was to establish an assay to evaluate sperm cell DNA integrity, due to the fact that there are several lines of evidence that sperm DNA damage leads to lower fertilization rates, disturbed embryo development and early abortions. The mitochondrial DNA is more susceptible than genomic DNA to DNA damage (Sawyer *et al.*, 2003; Yakes and Van1997). Based on this we hypothesise that mt-DNA has potential to act as a proxy for sperm cell genomic DNA integrity, with higher sensitivity that investigating the nuclear sperm genome itself. By taking advantage of PCR methods (quantitative PCR (QPCR) and long fragment PCR), we aim to detect DNA lesions caused by exposure to environmental agents.

The polymerase chain reaction is widely known for being a fast and simple tool to greatly amplify DNA. Although a powerful tool, it depends on several factors, one of which is the ability for the DNA polymerase to effectively incorporate new bases to the ever growing amplification products. If the DNA template that is being read by the DNA polymerase contains DNA lesions, the DNA polymerase may fall off, be permanently halted, leading to reduced progression speed. Such inhibition may be taken advantage of and allows for the polymerase chain reaction to be used as a tool for detecting DNA damage.

In order to measure the spontaneous levels of mt-DNA damage it is necessary to analyse a large fragment of the mitochondrial DNA, the longer the fragment amplified, the higher number of DNA lesions within the fragment may be detected. This amplified sequence was 10 kb of the total 16.5 kb mitochondrial genome. This 10 kb fragment is large enough to incorporate at least one “hit” when being exposed to environmental chemicals at relevant exposure levels (Santos *et al.*, 2006). This mt-DNA PCR will be referred to as the long mt-PCR assay or long fragment mt-PCR method onwards.

A Real-Time PCR for a small mt-DNA fragment (117 bp) was used in establishing the method for calculating the number of mitochondrial templates in each sample. The 117 bp

mitochondrial fragment is assumed to be too small to contain any spontaneous inhibiting DNA lesions or to receive any "hits" following environmental exposure, and will therefore act as a measure of mitochondria template concentration within each sample.

3.1.1 Determination of a suitable protocol for DNA isolation from mouse liver tissue.

We initially isolated DNA from mouse liver by using the agent DNAzol. This method of isolation was reported as a highly efficient, quick and suitable for conventional short PCR experimentation (Chomczynski *et al.*, 1997). Moreover using DNAzol was also reported as a DNA isolation method without spuriously induced oxidative damage due to the DNA isolation method itself, a well-known challenge when quantifying oxidative DNA damage (Mangal *et al.*, 2009). We consistently failed to produce adequate measurements on both the short- and long PCR assays, believed to be caused by the high protein and salt contaminations within our samples. Inspired by previous work measuring DNA damage in cells by PCR methods (Santos *et al.*, 2006), we tested an isolation method based on anion-exchange columns. This alternative DNA isolation procedure was the QIAGEN blood and cell kit, which greatly increased the purity of DNA in our samples, and consistent results were observed in the PCR assay.

3.1.2 Establishing suitable DNA quantification methods for determining template concentrations.

A very important step in the establishment of the assay was accurate and stable quantification of the amount of DNA in each reaction, which is a prerequisite for making comparisons of the amount of PCR-products between reactions. In this assay very low levels of DNA are used as template, making the DNA quantification more challenging. As it was highly important to trust the data that was presented when measuring DNA concentrations, a series of tests were done to attempt to clarify which method was most accurate with acceptable variation.

DNA standards were measured using two methods based on different principles; spectrophotometrical determination using the Nanodrop 1000 instrument and fluorometric

determination using the Qubit Fluorometer. Each standard was measured using 3 technical replicates.

The Qubit Fluorometer gave more accurate and consistent measurement compared to the Nanodrop (table 1).

Table 1. Comparisons of DNA quantification methods.

Sample DNA	Qubit measurements (ng / µl)		Nanodrop measurements (ng / µl)	
	Mean	SD +/-	Mean	SD +/-
lambda DNA 0.01 ng / µl	0.01	0.00	-0.23	0.52
lambda DNA 0.10 ng / µl	0.09	0.00	0.40	0.32
lambda DNA 1.0 ng / µl	0.92	0.00	1.64	0.35
lambda DNA 5.0 ng / µl	4.53	0.01	3.67	0.15
lambda DNA 25.0 ng / µl	22.0	0.00	20.05	0.80
lambda DNA 50 ng / µl	49.5	0.25	43.99	1.58

3.1.3 Optimizing the short mt-PCR assay.

With respect to the annealing temperature previous work done in our lab had established a temperature of 60 ºC as suitable for the reaction for the 117 bp amplicon. The presence of one unique PCR-product was determined by including a heat-denaturation step following the PCR amplification and by running conventional agarose gel analyses (figure10).

Complete denaturation of the template is important to obtain accurate and repeatable results. Two denaturing times of 6 and 10 min assumed to be long enough to separate both DNA strands efficiently, were compared. Eighteen liver samples (four *Ogg1*$^{-/-}$ (BO) and fourteen wild type (B) animals) were tested with the two annealing temperatures (figure 1). The mitochondrial DNA molecule is circular, and the denaturation step is important for the efficiency of the PCR amplification since it is well-known that there is different efficiency of PCR for circular template such as plasmids being supercoiled, relaxed or linearized (Chen *et al.*, 2007).

A very small, although significant difference in Ct-values were observed when comparing the denaturation times in wild type liver samples (Table 2), whereas no significant difference was observed in the four Ogg1-/- liver samples. We concluded that a denaturing time of 6 min was sufficient for the short mt-QPCR assay. Moreover, no significant difference between the Ct-values of Ogg1-/- and wild type mice with either the 6 or 10 min denaturation times (figure 1, Table 2; P = 0.05), indicating similar numbers of mitochondrial DNA molecules per ng total DNA in both genotypes. The deficiency in *Ogg1*$^{-/-}$ thus did not lead to changes in number of mitochondrial DNA molecules per cell.

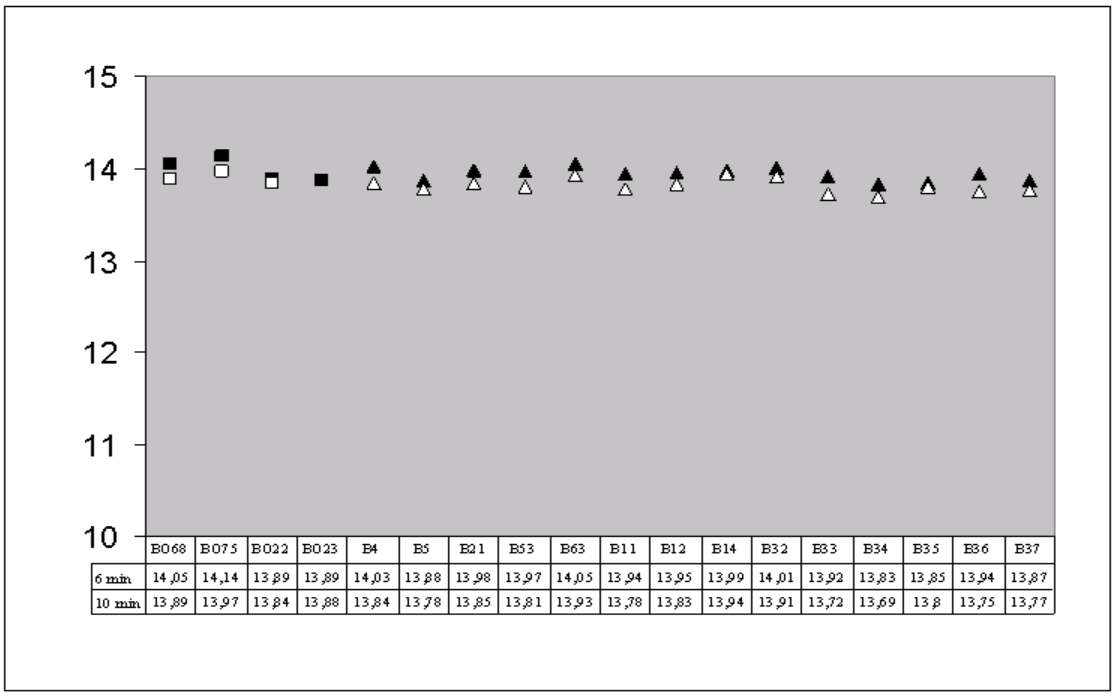

	B068	B075	B022	B023	B4	B5	B21	B53	B63	B11	B12	B14	B32	B33	B34	B35	B36	B37
6 min	14,05	14,14	13,89	13,89	14,03	13,88	13,98	13,97	14,05	13,94	13,95	13,99	14,01	13,92	13,83	13,85	13,94	13,87
10 min	13,89	13,97	13,84	13,88	13,84	13,78	13,85	13,81	13,93	13,78	13,83	13,94	13,91	13,72	13,69	13,8	13,75	13,77

Figure 1. Evaluation of denaturing times for the Real Time 117 bp mt-QPCR assay in liver DNA from *Ogg1*$^{-/-}$ and wild type mice. Denaturing times of 6 and 10 min were compared in *Ogg1*$^{-/-}$ liver DNA (■- 6 min, □ – 10 min) and wild type liver DNA (▲- 6 min, Δ – 10 min). The PCR amplification is indicated using Ct-values, and the values for each sample along with the name of the mice tested are indicated below in a table. Note that the Y-axis omits values below 10, for clarity.

Table 2. Comparison of mean Ct values for 6 and 10 min denaturation times in the short mt-QPCR assay in liver DNA from *Ogg1*$^{-/-}$ (BO) and wild type (B) mice.

	6 min	10 min	Difference	*P-value
BO, mean Ct +/- SD	13.99 +/- 0.12	13.90 +/ -0.05	0.09 +/- 0.13	0.20
B, mean Ct +/- SD	13.94 +/- 0.06	13.81 +/- 0.08	0.13 +/- 0.10	0.0001

* Calculated by using Students t-test.

3.1.4 Efficiency of the short mt-QPCR assay.

To verify that the amplification of the short 117 bp amplicon was not affected by the exposure level of B(a)P used in this work and to investigate the efficiency of the mt-QPCR assay a series of DNA starting template concentrations were tested. Two liver DNA samples, one from an unexposed mouse and one from a B(a)P-exposed wild type mouse were tested, using two different starting concentrations of 3 ng / µl and 5 ng / µl (figure 2 and 3). Five dilutions were tested (1:1, 1:10, 1:100, 1:1000 and 1:10000), each with four replicates.

The efficiency of the reaction was evaluated by product formation vs. dilution factor. It was therefore necessary to establish the linear regression of each reaction. Linear regression values range between 0 and 1, and a value close to 1 indicates linearity.

When excluding the 1:1 dilution that were not linear with the other dilutions tested in one of the samples (figure 2), linear regression coefficients of 0.99 were obtained for all four reactions (fig 3). On basis of this it was decided to exclusively use the 1:10 dilution in all future short mt-QPCR experiments.

The linearity of the B(a)P-exposed samples verified that no “hits” were introduced into the 117 bp region. The standard deviations among replicates of each sample were below 1 % and were therefore not included in the graphs for clarity.

Lower Ct-values was observed in samples containing 5 vs 3 ng / µl starting concentration throughout the whole range of tests, showing that the higher number of starting templates was reflected in the Ct values. The 3 ng / µl samples had on average a 1.28 (control) or 1.38 (exposed) higher Ct value than the 5 ng / µl, confirming that less starting DNA was present.

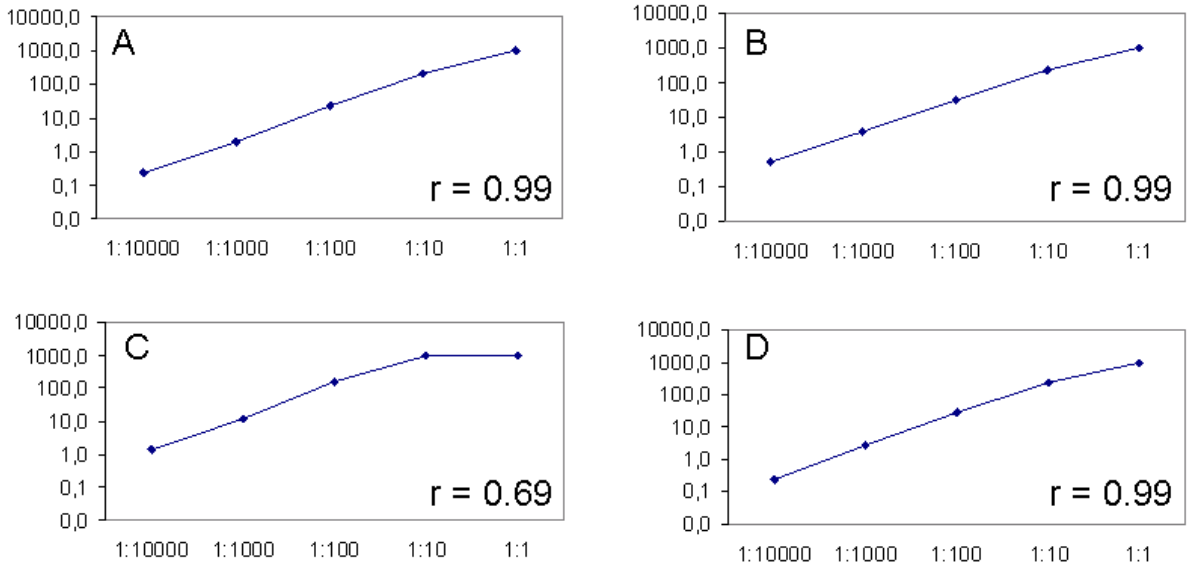

Figure 2. Efficiency of the 117 bp short Real Time mt-QPCR assay in liver DNA samples. Relative PCR amplification of the 117 bp fragment is shown on the Y axis. This is relative only to its own dilutions, and has no relationship with the other graphs listed. The X-axis shows the dilutions of template tested. **A)** Control liver DNA, 3 ng / µl. **B)** Control liver DNA, 5 ng / µl. **C)** B(a)P-exposed liver DNA, 3 ng / µl. **D)** B(a)P-exposed liver DNA, 5 ng / µl.

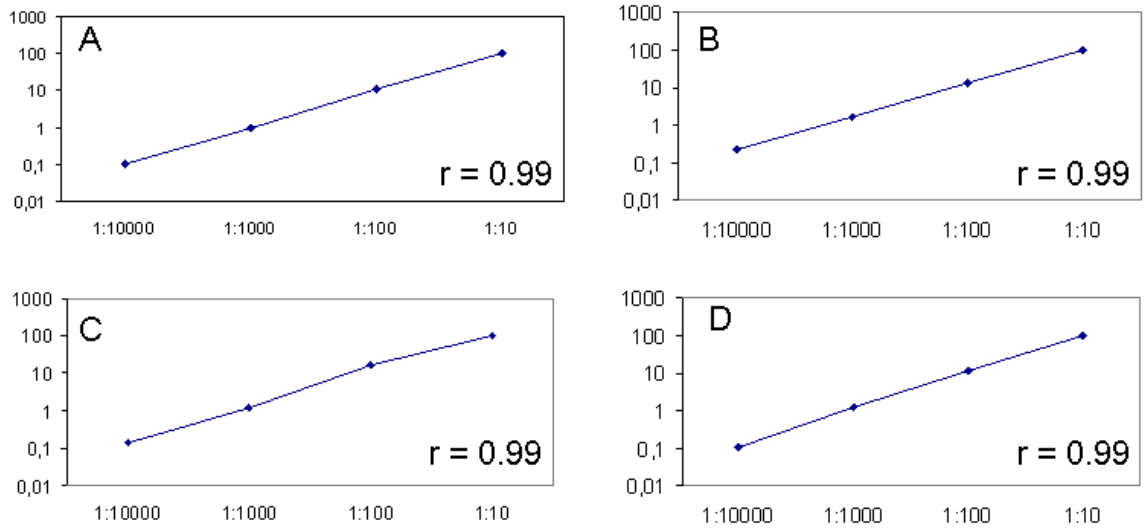

Figure 3. Efficiency of the 117 bp short Real Time mt-QPCR assay in liver DNA samples (excluding the 1:1 dilution). Relative PCR amplification of the 117 bp fragment is shown on the Y axis. This is relative only to its own dilutions, and has no relationship with the other graphs listed. The X-axis shows the dilutions of template tested. **A)** Control liver DNA, 3 ng / µl. **B)** Control liver DNA, 5 ng / µl. **C)** B(a)P-exposed liver DNA, 3 ng / µl. **D)** B(a)P-exposed liver DNA, 5 ng / µl.

3.1.5 Optimizing the long mt-PCR assay.

The long mt-PCR assay was run by conventional PCR using a PCR kit (XL PCR) suitable for amplification of long amplicons. Determination of a suitable annealing temperature was done by running a temperature gradient during the PCR on DNA isolated from liver tissue from a wild type mouse. The DNA was isolated using QIAGEN columns. The DNA was sequentially diluted to a final concentration of 5 ng / µl. Other variables besides annealing temperature including amount of DNA template and presence of DNAse-free bovine serum albumin (BSA) were tested. The results were concluded visually by running 0.7 % agarose gels (figure 4).

The results shows the presence of a single PCR product and indicated that samples containing BSA and a DNA dilution of 1:10, with an annealing temperature of 64 ºC gave highest amplification (wells 10-11) when determined by measurement on the Qubit Fluorometer (data shown in Appendix A).

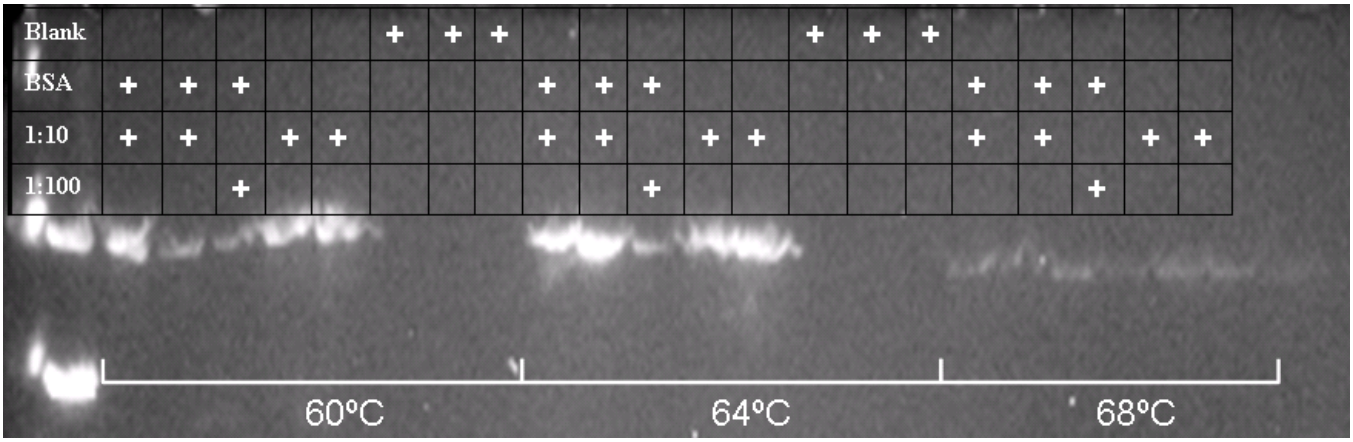

Figure 4. Optimization of the 10 kb long mt-PCR assay. The gel shows single 10 kb bands in each lane from long mt-PCR amplifications of liver tissue DNA samples at different annealing temperatures. The DNA samples contained 5 ng / µl DNA diluted 1:10 or 1:100. The presence of BSA was tested and blanks are presented as indicated above each lane. Blanks at 68 ºC were not included on this gel due to lane restrictions. The lane furthest to the left contains a 1 kb ZipRuler ladder.

3.2 Establishment of the mitochondrial DNA damage assay (MDDA) in cultivated cells or frozen tissues from mice.

Before embarking on *in vivo* mouse experiments with freshly harvested cells and tissue, the MDDA method was established in cultured cells and frozen tissues to ensure that the long and short mt-PCR assays were suitable for detection of mitochondrial DNA damage.

3.2.1 MDDA on DNA from cells exposed to H_2O_2 *in vitro*.

Perhaps best known for its ability to generate 8-hydroxydeoxyguanosines, hydrogen peroxide also generate a substantial amount of other types of oxidized DNA lesions (Termini 2000). Not all oxidized DNA lesions inhibit the progression of DNA polymerases (Santos *et al.*, 2006), but the diverse set of lesions induced by H_2O_2 was suitable for the purpose of assay testing. Hydrogen peroxide was therefore chosen as a model compound that would promote high levels of DNA damage and give a high chance of producing a plethora of DNA lesions including DNA lesions that inhibits DNA polymerases, that could detected by MDDA.

Cells were exposed *in vitro* to three high concentrations of H_2O_2 (100 μM, 400 μM, 800 μM), along with an unexposed control sample. Results using the long mt-PCR assay showed the presence of one unique amplification product (figure 5). Densitometric analysis of the gel provided data about the amplification of the 10 kb fragment.

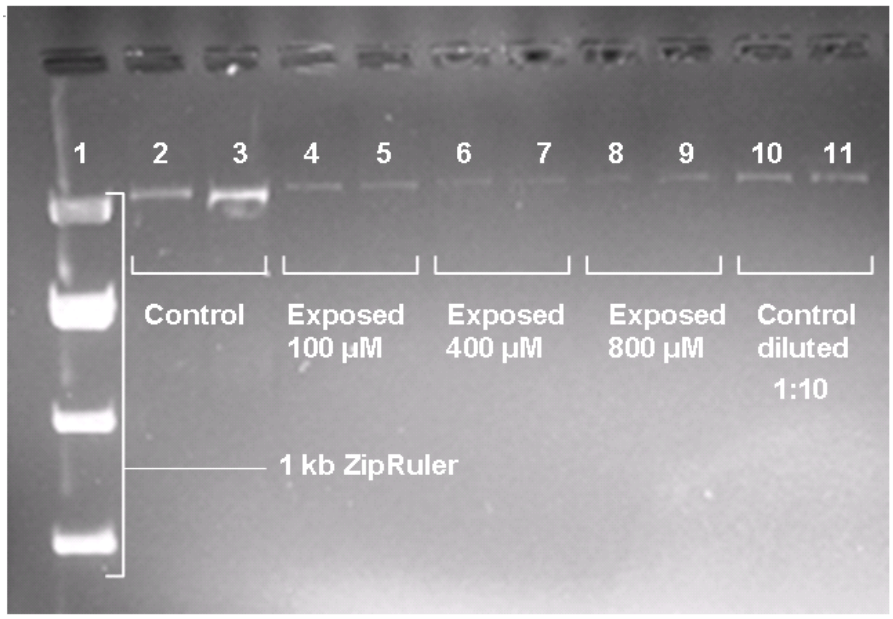

Figure 5. Gel photo of long mt-PCR products from liver cells (Hepa1c1c7) exposed to hydrogen peroxide *in vitro*. The gel shows the 10 kb mitochondria fragment amplified from DNA isolated from liver cells exposed to different concentrations (0, 100, 400 and 800 µM) hydrogen peroxide for 1 hour. Well 1: ZipRuler 1 kb DNA; 2-3: undiluted unexposed sample; 4-5: exposed 100 µM; 6-7: exposed 400 µM; 8-9: exposed 800 µM and 10-11: diluted (1:10) unexposed sample.

The short mt-QPCR assay was used to assess if there had been any changes to the number of mitochondrial molecules per ng DNA due to exposure. The exposed cells showed a dose-dependent significant decrease in mitochondrial genome numbers; from 100% in the unexposed samples to 36, 62 and 74 %, all with SD lower than 2 % (figure 6A). The loss of mitochondria template was highly significant throughout all concentrations. All between dose comparisons were also highly significant (* $P < 0.0001$).

Assessment of DNA damage by the MDDA assay was performed in these cells. Densitometric analyses of the gel images provided data about the amplification of the 10 kb fragment. After adjusting for the loss of mitochondria the exposed cells showed a relative amplification of 17, 26 and 34% (SD +/- 0.4, 0.5 and 0.7 %, respectively) when compared to the control (SD +/- 5.7%) (figure 6B). No statistical analysis of significance at this stage was attempted due to low number of technical replicates.

This translates to 1.77, 1.35 and 1.08 lesion per 10 kb, respectively

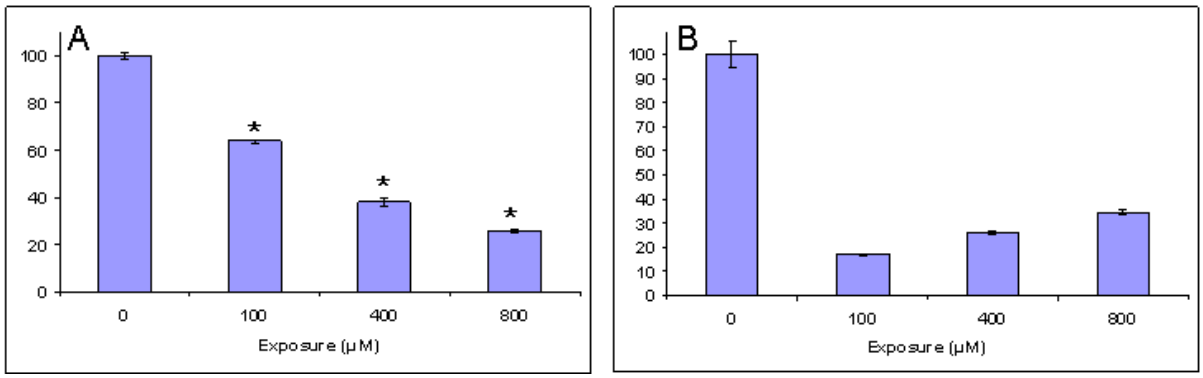

Figure 6. Assessment of mitochondrial genome numbers and mitochondrial DNA damage levels in liver cells (Hepa1c1c7) exposed to hydrogen peroxide *in vitro*. A: Loss of mitochondrial genome numbers in liver cells (Hepa1c1c7) due to *in vitro* exposure to hydrogen peroxide. Representation of fluorescence values (n=8) obtained after Real Time PCR amplification of the 117 bp mitochondrial fragment of liver cells exposed to different hydrogen peroxide concentrations. Values are log transformed, relative to the control, to percent. * = P < 0.0001. B: Mitochondrial DNA damage levels in Hepa1c1c7 liver cells after *in vitro* exposure to hydrogen peroxide. The bars indicate values (percent of unexposed samples) determined densitometriccally by the values (n=2) of the 10 kb mitochondrial fragments formed using the long mt-PCR assay that have been adjusted relative to template number (presented in A).

3.2.2 Frozen liver tissue from mice exposed to B(a)P *in vivo*.

Frozen tissue typically contains higher amounts of DNA damage than fresh tissue (Fairbairn *et al.*, 1994). If high background levels of DNA damage were induced due to freezing one would expect a reduction in the sensitivity of the method and more uniform amplification of DNA irrespective of exposure level. We initiated an experiment to address these issues and to measure mitochondrial DNA damage levels in different DNA samples.

Three samples were used for this experiment, one of which was a knockout animal for the gene *OGG1*, which encodes a protein involved in repair of DNA lesions, more specifically in base excision repair. The mice were exposed to B(a)P (3 x 50 mg/kg bw, total 150 mg/bw, on three consecutive days). Samples were from a previous experiment, and had been frozen at -80 ºC for several months.
The three liver samples were taken from:

- One unexposed wild-type (B55).
- One B(a)P-exposed wild-type (B23).
- One unexposed Ogg1$^{-/-}$ (BO46).

The unexposed Ogg1$^{-/-}$ mouse (BO46) had the lowest Ct value, and the values for the other two samples are expressed relative to this (figure 7A). The exposed wild-type (B23) had the highest Ct value, which when linearized was equal to a loss of 23.4 % starting template, with a SD of +/- 1 %. This difference in mitochondrial template was shown to be highly significant (* P< 0.002). The unexposed wild-type (B55) was determined to have a loss of 7.9 % starting template, SD +/- 1 % (figure 7A). There was no significant difference between this sample and the unexposed knockout.

Mitochondrial DNA damage levels presented in figure 7B is based on the densitometric analysis of the gel on the amplification of the 10 kb fragment (Figure 8) relative to the amount of mitochondrial DNA template (figure 7A). The unexposed wild-type (B55) had the most efficient amplification of PCR-product, which was defined as 100 %, SD +/- 30 %. When comparing the unexposed KO (BO46) and exposed wild-type (B23) animals to this value, a reduction of 13 and 17 % was observed, SD +/- 8 and 41 % (figure 7B). Considering the variations observed between replicates of each sample, no significant differences were evident. This resulted in a lesion frequency per 10 kb ratio of 0.13 for the unexposed KO and 0.18 for the exposed wild-type.

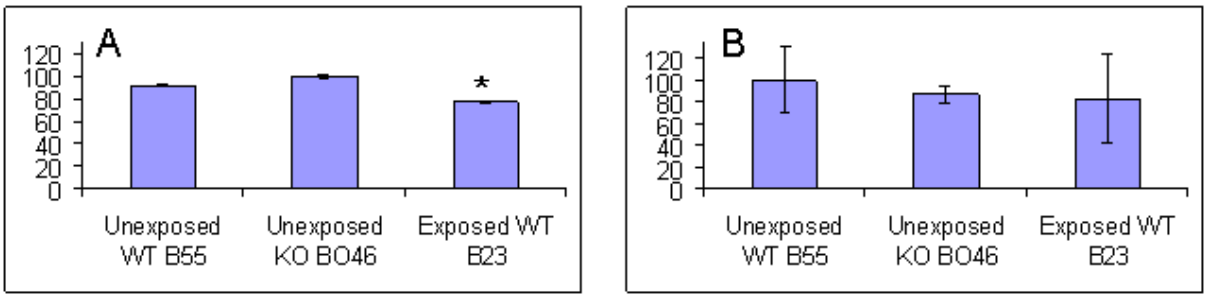

Figure 7. Assessment of mitochondrial genome numbers and mitochondrial DNA damage levels in frozen liver of mice. A: Mitochondrial template numbers in DNA from frozen livers of one unexposed wild-type, one unexposed Ogg1$^{-/-}$ and one B(a)P exposed wild-type mouse. Representation of fluorescence values (n=6) obtained after Real Time PCR amplification of the 117 bp mitochondrial fragment of frozen Hepa1c1c7 liver cells. Values are log transformed, relative to the control, to percent. B. Mitochondrial DNA damage levels in frozen liver following exposure to B(a)P. The bars indicate values (percent of control sample) determined densitometriccally by the values (n=2) of the 10 kb mitochondrial fragments formed using the long mt-PCR assay that have been adjusted relative to template number (presented in A).

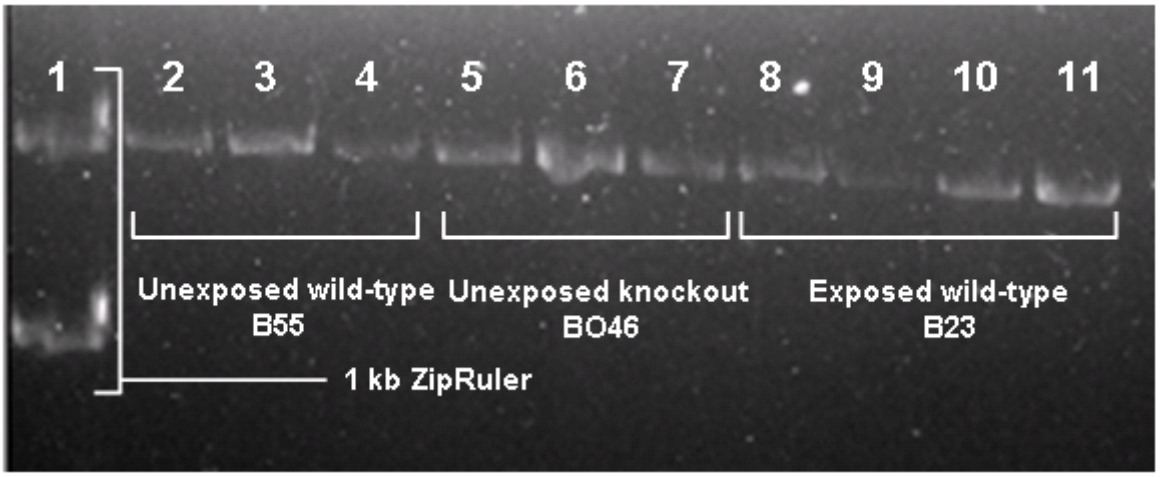

Figure 8. Gel photo of long mt-PCR products from frozen liver cells exposed B(a)P. The gel show the 10 kb mitochondria fragment amplified from DNA isolated from frozen liver cells. Well 1: ZipRuler 1 kb DNA; 2-4: unexposed wild-type; 5-7: unexposed Ogg1$^{-/-}$; 8-11: B(a)P exposed wild-type.

3.3 Detection of mitochondrial DNA damage in mice after *in vivo* exposure to B(a)P.

The established MDDA-assay were used for detecting mitochondrial DNA damage in freshly harvested sperm and liver of mice following *in vivo* exposure to B(a)P. B(a)P exposed mice received one injection (150 mg/kilo, i.p.) four days prior to sacrifice, while the unexposed animals received an equivalent volume of phosphate buffered saline (PBS)

Four separate biological experiments were performed, each consisting of one control male and one B(a)P exposed male.

3.3.1 DNA damage in somatic cells: liver.

Typical results from the long PCR assay (figure 9) and short PCR assay (figure 10) are shown below. The use of freshly harvested tissue greatly enhanced the efficiency of the long PCR assay, verifying that freezing of tissue induces fragmentation of the mitochondrial DNA template.

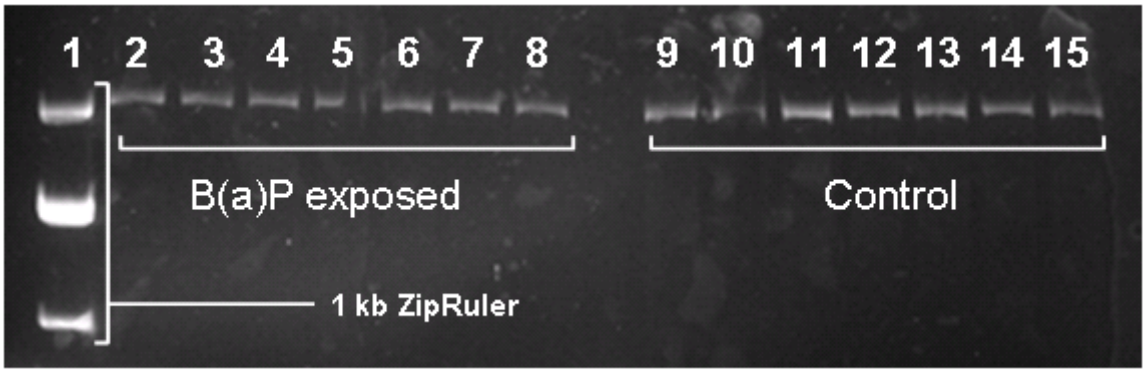

Figure 9. A typical gel photo, showing a clear row of the 10 kb PCR-product from B(a)P exposed and unexposed wild type samples. Densitometric analysis was used to calculate the band strength of each lane.

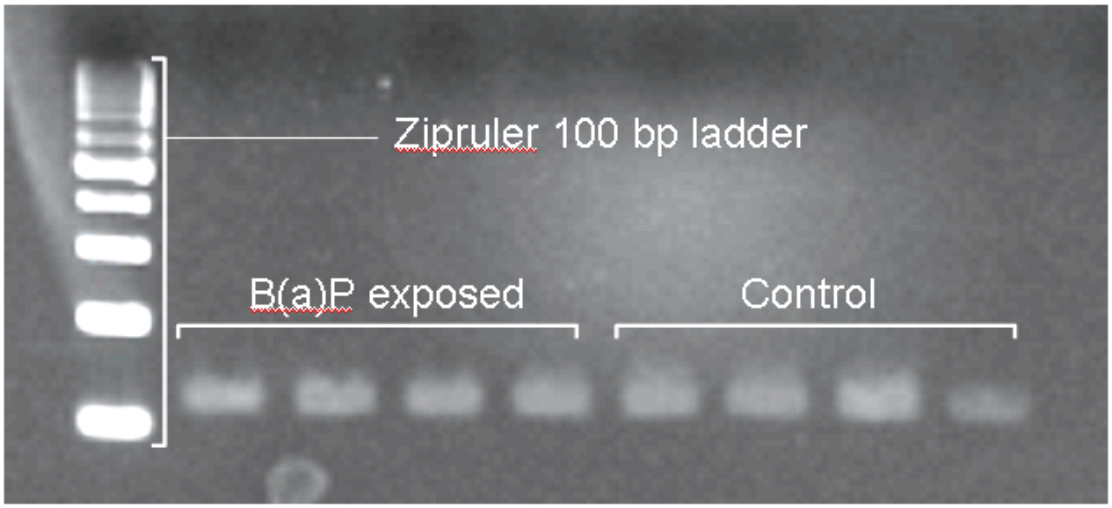

Figure 10. Gel image of a 2.2 % FlashGel showing the 117 bp PCR product between the ZipRuler 100 and 200 bp ladder bands.

The results onwards are from four separate biological experiments, each consisting of one control male and one B(a)P exposed male. The results are tabulated in Table 3 and presented graphically in figure11.

Table 3. Summary of results from four experiments of B(a)P exposure to mice. Liver tissue is used for extraction of DNA. Shown are the reductions in mt template obtained from the short PCR assay, the uncorrected levels of mt-DNA damage in the long PCR assay shown by densitometric analysis, and the corrected mt DNA damage levels after adjusting for the loss of mitochondria. Also listed are the lesions per 10 kb ratio before and after adjusting for loss of mitochondrial template.

	Reduction in mt template, %	Uncorrected mt DNA damage level	Lesions per 10 kb, uncorrected	Corrected mt DNA damage level, %	Lesions per 10 kb, corrected	Corrected unexposed control, %
Exp 1	15 +/- 1	31	0.37	20 +/- 15	0.22	100 +/- 10
Exp 2	23 +/- 1	20	0.22	2 +/- 15	0.02	100 +/- 15
Exp 3	14 +/- 1	34	0.42	23 +/- 17	0.26	100 +/- 16
Exp 4	19 +/- 1	57	0.84	29 +/- 60	0.34	100 +/- 37
Mean	18 +/- 4	36 +/- 16	0.46 +/- 0.26	19 +/- 12	0.21 +/- 0.14	100

The number of mitochondrial templates per ng total DNA were consistently lower in B(a)P-exposed compared to unexposed mice, ranging from 14-23 % decrease with a mean of 18 %, SD +/- 4 %. This loss in mitochondrial templates was shown to be highly significant (*$P < 0.0001$). Moreover, with the exception of one experiment (Exp 2) the level of mitochondrial damage as assessed by MDDA was consistently higher in B(a)P-exposed mice than in unexposed mice, ranging from 20 – 29 % higher giving a mean of 24 %, SD +/- 5. The levels of mitochondrial damage related to amount of DNA used as template without correcting for the amount of mitochondrial template molecules per ng DNA was 36 %, SD +/- 16%.

Rather high levels of variation were observed among replicates.

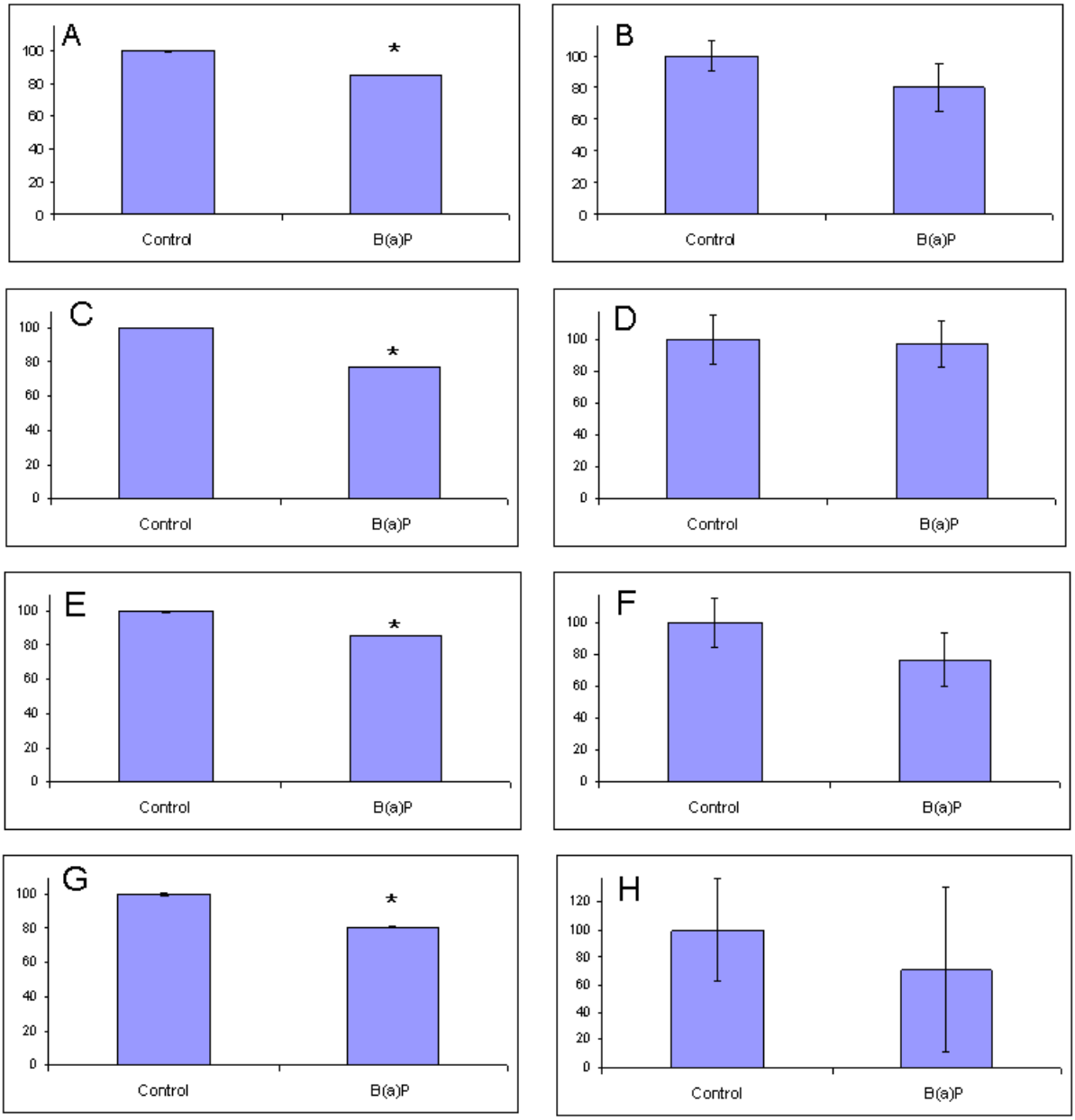

Figure 11. Mitochondrial template numbers and DNA damage levels in freshly harvested liver tissue of mice exposed to B(a)P. The results are from four biologically distinct experiments denoted Exp1-4. The number of mitochondrial templates in the liver DNA samples of the four experiments are indicated in A, C, E and G. This loss in mitochondrial templates was shown to be highly significant (*P < 0.0001). The results are obtained by short mt-QPCR of 117 bp and are presented as percentages of the unexposed control mice in each experiment. The amount of mitochondrial DNA damage in each experiment is shown in B, D, F and H. The values represented are based on densitometric analysis of the 10 kb mitochondrial PCR products formed using the long PCR assay relative to the number of mitochondrial template molecules in each sample. The percentage of damage was presented as percentages of the unexposed control sample.

3.3.2 DNA damage in male germ cells: sperm.

Our main aim was to establish a simple method for measuring mt-DNA integrity in sperm.

The first challenge to overcome was to develop a suitable protocol for isolating sperm mitochondrial DNA, without introducing new DNA damage due to the isolation protocol itself. Due to the inherent challenge of isolating high molecular genomic sperm DNA a novel method based on very simple principles was developed.

In general, conventional methods for DNA isolation from tissues (QIAGEN blood and cell culture kit and DNAzol) were unsuccessful in sperm cells. A novel method for sperm cells was established: due to the fact that the sperm mitochondria are located separate from the nuclear DNA, in the tail region of the sperm, mitochondrial DNA could be released from sperm separately.

In the initial protocol of the Sperm Mitochondrial DNA Extraction (SMD) method was very simple. Making use of a detergent (Triton-X) to resolve the tail structure and the mitochondrial membranes to simply release the mitochondrial DNA molecules within followed by separation of the mitochondrial DNA molecules from the remaining sperm by filtration using gauze. The DNA obtained was suitable for short PCR assays, and optimization of the percentage of Triton-X was established with the short mt-QPCR assay as functional assay. Attempts were made to run the long mt-PCR assay on this DNA, without success. Mitochondrial DNA molecules are known to be associated to the inner membrane of the mitochondria, and it was likely that protein molecules were still associated with the isolated DNA molecules or the isolates contained proteins that inhibit the long mt-PCR assay. Including a step in the protocol for digesting proteins, using Proteinase K, resolved the challenge of making the long mt-PCR assay work. The DNA was precipitated using ethanol giving concentrations of DNA of 10-20 ng / µl.

The short mt-QPCR assay was used on DNA isolated by the SMD including Proteinase K digestion from six biological samples (three wild-type and three Ogg1$^{-/-}$ mice) including six technical replicates for each sample (figure 12). The Ct values obtained varied considerably between the mice, clearly showing that the extraction protocol still warrants further

development. The Ct values for wild type mice varied from 19.3 to 34.9, which translates to a difference of 50 000 times in starting mt-DNA template concentration. The amount of total DNA in all samples was 5 ng / µl. The standard deviation for each wild type sample varied from 0.8 to 5.4. Ct values for the Ogg1-/- mice varied from 19.1 to 29.1, translating to a difference of 1000 times in starting mt-DNA template. For these samples all samples started with 5 ng / µl that were diluted 1:10. The standard deviation varied from 0.2 to 2.4.

The long mt-PCR assay was successful for sperm mitochondrial DNA using the SMD method with Proteinase K digestion with a single amplification product of 10 kb (Figure 13). Although no consistency between the samples was observed, liberal interpretation of the results presented in figure 12 indicates that there may be higher levels of PCR-amplification in wild-type compared to Ogg1-/- mice.

As the SMD method clearly warrants further optimization that was beyond the scope of this MSc thesis, no correlation between exposure and amplification values were observed.

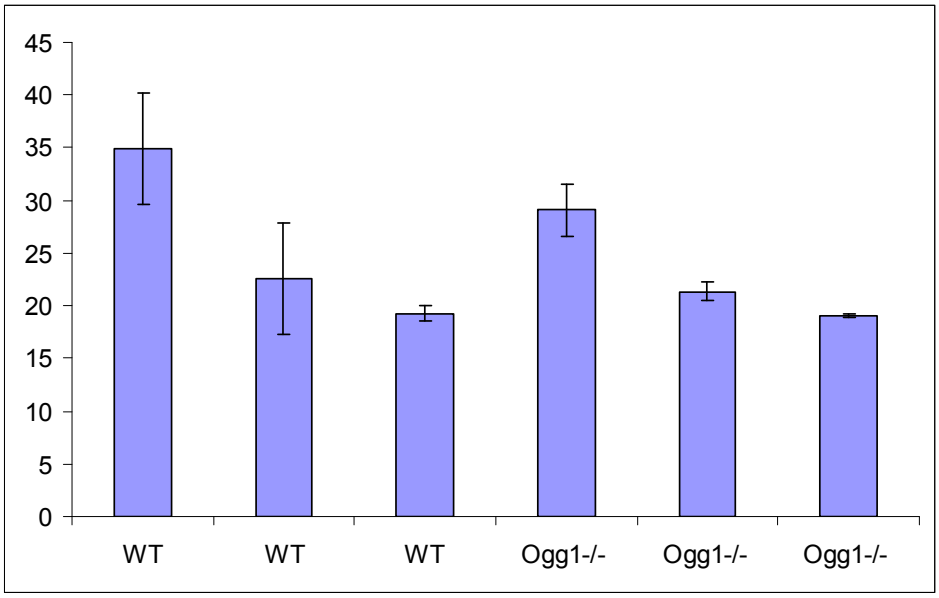

Figure 12. Short mt-QPCR assay on DNA isolated from freshly harvested sperm of mice. The number of mitochondrial DNA molecules is indicated as Ct values on the y-axis, and the genotype of the mice that sperm DNA was isolated from (either Ogg1-/- or WT) is indicated on the x-axis. The results are presented as means of six technical replicates for each sample and the error bars represents standard deviations to the means.

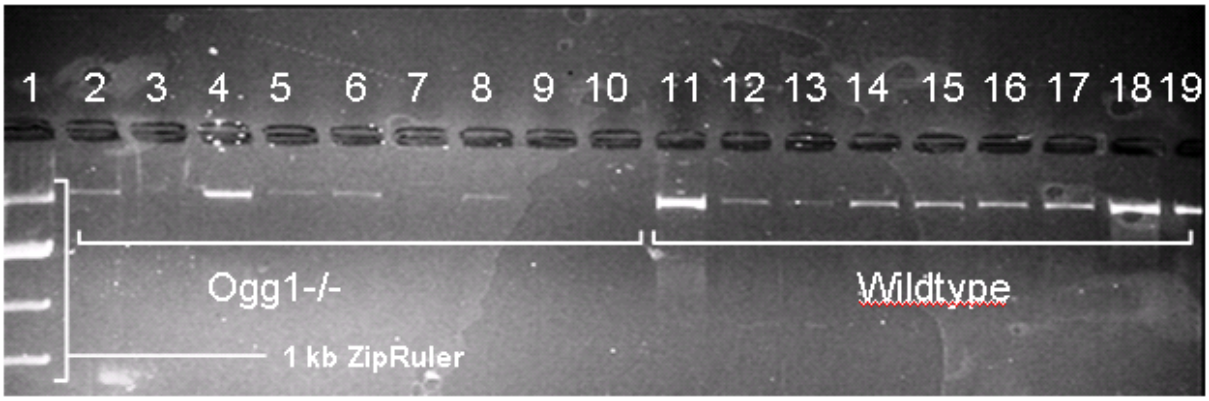

Figure 13. Three technical replicates of samples listed in figure 12. Long mt-PCR on DNA isolated from freshly harvested sperm of wild-type and Ogg1-/- mice. This is an image of an agarose gel of the single PCR product of sperm mtDNA of 10 kb. Well 1: ZipRuler 1 kb DNA; 2-4: unexposed Ogg1-/-; 5-7: unexposed Ogg1$^{-/-}$; 8-10: unexposed Ogg1-/-; 11-13: unexposed wild-type; 14-16: unexposed wild-type; 17-19: unexposed wild-type.

3.5 Effects of paternal exposure to B(a)P or and GA on fertilization and early embryo development.

Reduced fertility within males has been observed over the last decades, most notably in industrialized countries (Auger *et al.*, 1995; Carlsen *et al.*, 1992). It is therefore assumed that factors of our lifestyle, such as diet and environment, are direct causes implicated in this observation. Exposure to either B(a)P or GA are known to induce damage in DNA, as they and their metabolites bind covalently to deoxyadenosines and deoxyguanosines (Mensing *et al.*, 2005; Solomon *et al.*, 1985).

It has been demonstrated that paternal exposure to either chemical has the ability to be transferred, via sperm, to the next generation (Generoso *et al.*, 1996). We aimed at elucidating if high single exposures, although far below the lethal doses, of B(a)P or GA to males are involved in decreasing fertilization rates or disturbing early embryo development. This set of experiments are a part of a larger project, investigating the impact of sperm DNA lesions on fertilization, early embryo development, and miRNA and mRNA expression during early embryo development following fertilization with sperm from exposed mice.

3.5.1 Counting embryos at different developmental stages.

Exposure to Glycidamide:

To observe the impact of *in vivo* exposure on fertilization (progression to the 2-cell stage) eight fertilization experiments were performed. Each experiment contained 12 females and 2 males (one unexposed and one exposed to GA), with an average of 58 starting oocytes for control sperm and 75 for exposed sperm (figure 13).

Progression to the 2-cell stage, when using sperm from control animals, ranged between 32-92 %, with a mean rate of 57 %, SD +/- 19 %. For sperm that had come from animals exposed to GA, a progression to the 2-cell stage was between 18-54 %, with a mean rate of 40 %, SD +/- 22 %. A P-value of < 0.001 (*) showing that the fertilization rate is reduced when sperm is exposed to GA.

Qualified visual inspection of embryos were performed, and photos were taken at both different stages involved with fertilization and progression to the 2-cell stage (figure 14)

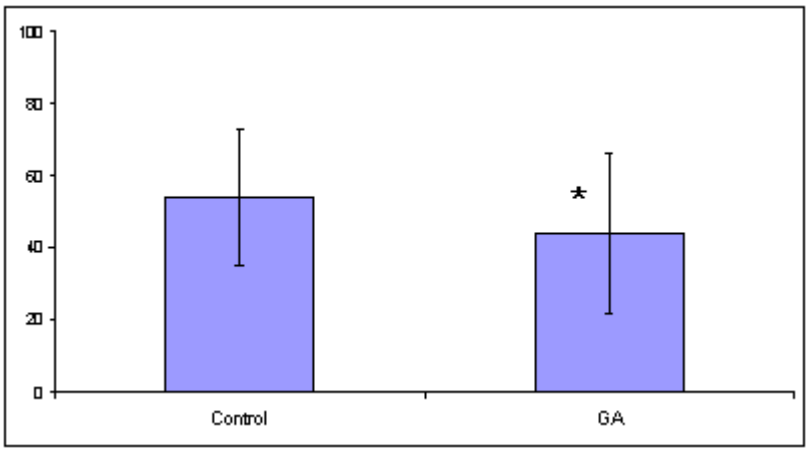

Figure 14. Fertilization rates for sperm from control and glycidamide exposed mice (*in vivo*). Values represent fertilization rates of sperm from control mice (n=464) vs. sperm from glycidamide exposed mice (n=600). Bars have been adjusted to percent.

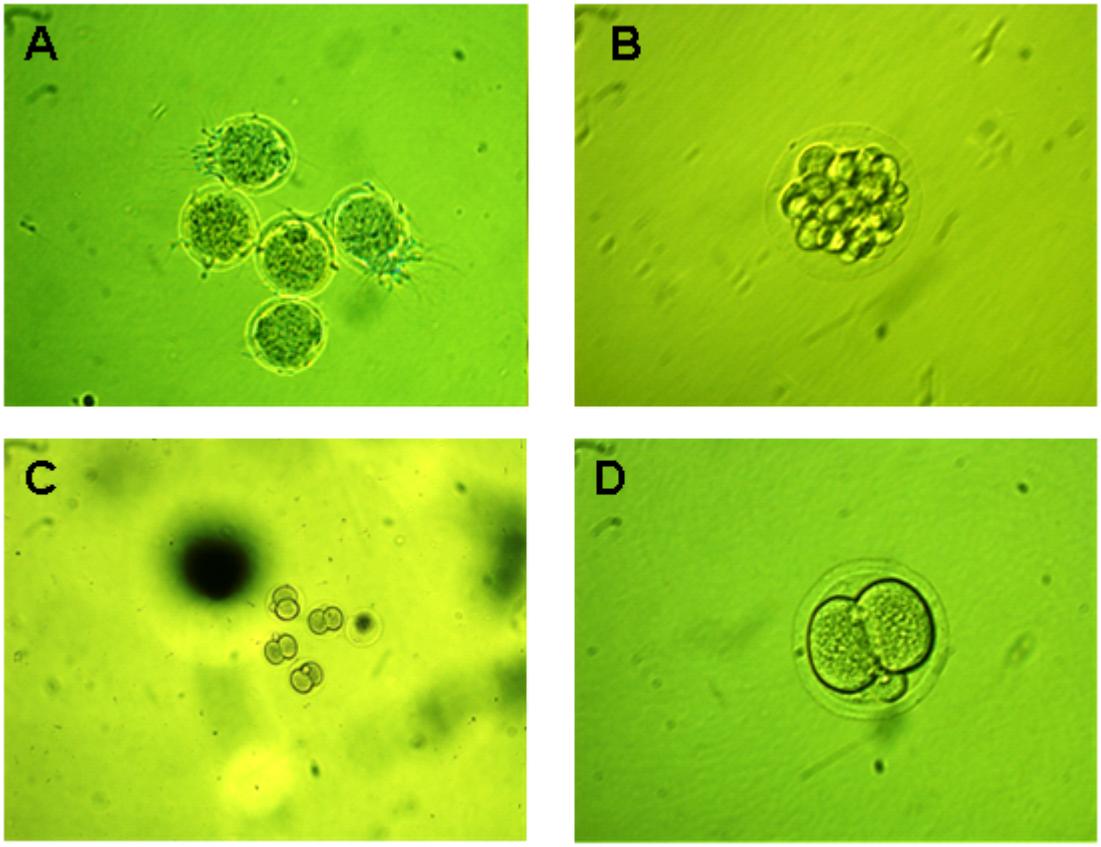

Figure 15. Fertilization and progression to the 2-cell stage. A) Fertilization of oocytes with sperm from GA-exposed mice. **B)** Fragmentation of embryo after unsuccessful fertilization. **C)** Embryos at 24 hours after fertilization. **D)** Higher magnification of 2-cell embryo.

Exposure to B(a)P:

To observe the impact of *in vivo* exposure on fertilization (progression to the 2-cell stage) three fertilization experiments were performed. Each experiment contained 12 females and 2 males (one unexposed and one exposed to B(a)P), with an average of 72 starting oocytes for control sperm and 61 for exposed sperm (figure 15).

Progression to the 2-cell stage, when using sperm from control animals, ranged between 80-88 %, with a mean rate of 85 %, SD +/- 4 %. For sperm that had come from animals exposed to B(a)P, a progression to the 2-cell stage was between 69-86 %, with a mean rate of 72 %, SD +/- 14 %. A Chi-square test on this difference in fertilization * gave a P-value of < 0.001 showing that the fertilization rate is reduced when sperm is exposed to B(a)P.

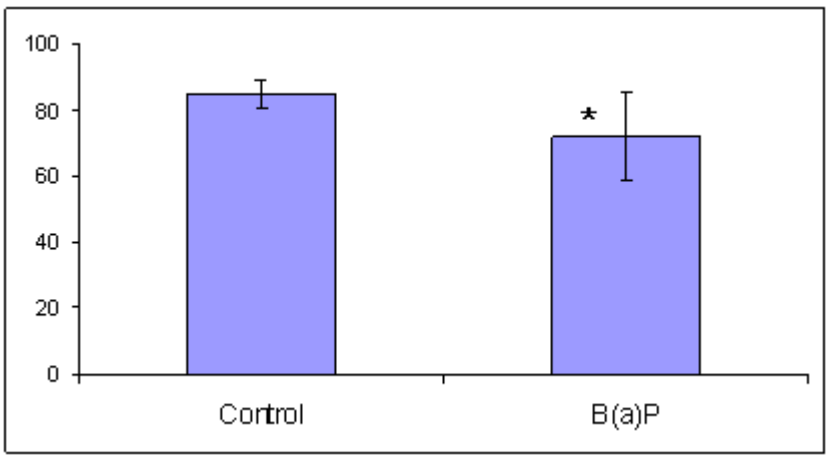

Figure 16. Fertilization rates for sperm from control and B(a)P exposed mice (*in vivo*). Values represent fertilization rates of sperm from control mice vs. sperm from B(a)P exposed mice. Bars have been adjusted to percent.

To observe the impact of *in vivo* exposure on fertilization and early embryonic development (progression to the 2-, 4- and 8-cell stage) two experiments were performed. Each experiment contained 12 females and 2 males (one unexposed and one exposed to B(a)P) with an average of 77 starting oocytes for control sperm and 64 for B(a)P exposed sperm (fig 16).

Progression to the 2-, 4- and 8-cell stage, when using control mice sperm decreased from 82 to 64 to 59 %, with a SD +/- 2, 5 and 10 % at the respective stages. For sperm that had been come from B(a)P exposed mice, progression to the 2-, 4- and 8-cell stage decreased from 75 to 61 to 56 %, with a SD +/- 9, 22 and 29 % at the respective stages. The results do not indicate any disturbance on early embryo development with respect to progression.

Qualified visual inspection of embryos were performed, and photos were taken at different stages involved with progression to the 2-, 4- and 8- cell stage (figure 17)

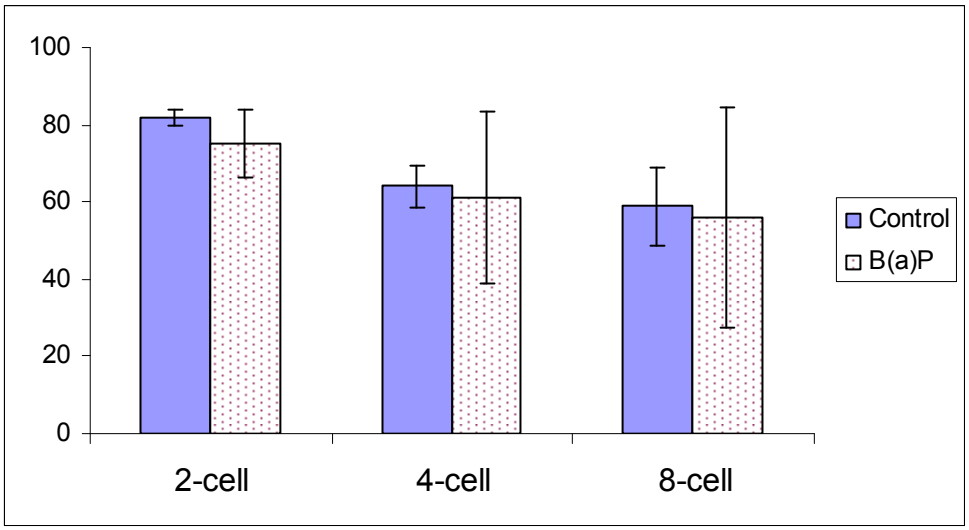

Figure 17. Early embryo development between sperm from control and B(a)P exposed mice (*in vivo*). Values represent fertilization rates of sperm from control mice (n=154) vs. sperm from B(a)P exposed mice (n=128). Bars have been adjusted to percent.

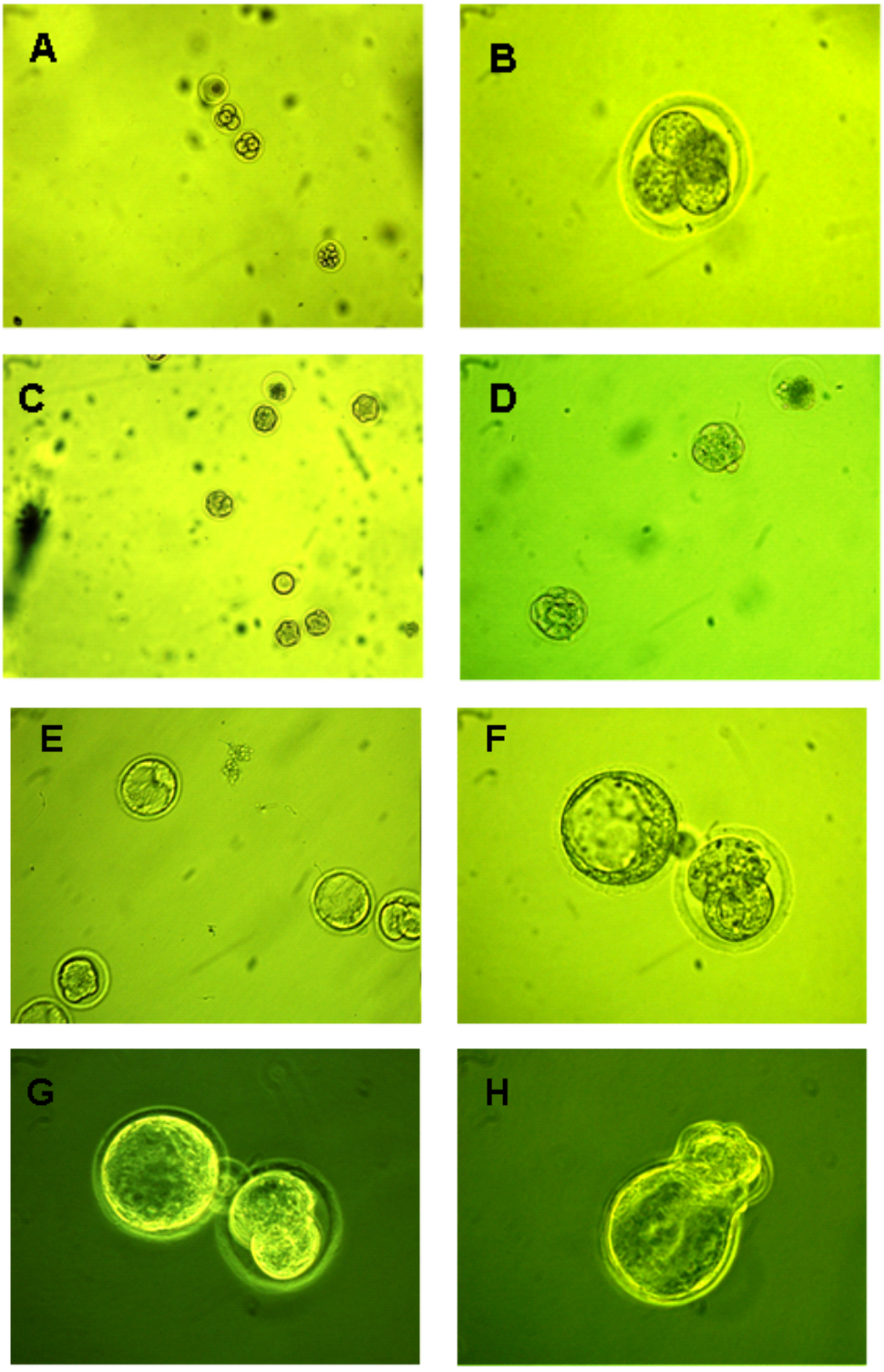

Figure 18. Early embryo development. **A)** Two embryos at the 4-cell stage, one unfertilized oocyte and one dead embryo. **B)** Higher magnification of 4-cell embryo. **C)** Five embryos at the 8-cell stage. **D)** 8-cell embryos can be recognized by their cloud shape structures. **E)** Embryos at the blastula stage. **F)** Blastulas are easily recognized by their fluid filled cavity known as the blastocoel. **G)** Embryos at the blastocyst stage. **H)** After the zona pellucida is lysed, hatching occurs, so that the blastocyst can be implanted on the uterine wall.

4. Discussion

This part has been divided into two sections. The first part deals with optimization of the methods required for experimentation. The second section discusses the results employing the methods discussed in part one.

4.1 The establishment of a short PCR and a long PCR assay for detecting DNA damage; the mitochondrial DNA damage assay.

Initial work by Ben van Houten (Van Houten B. *et al.*, 1998) established the long and short PCR methods for detection of cellular DNA damage, but no one has yet adapted this method for use on sperm cells. Previous work to detect DNA damage with techniques based on PCR have relied on a short fragment to estimate template concentration and a long fragment to detect lesions which halt the progression of the DNA polymerase during replication. This work are either successful in observing differences between exposed / control cells (Ayala-Torres *et al.*, 2000; Ballinger *et al.*, 1999; Kalinowski *et al.*, 1992; Laws *et al.*, 2001; Mattes1990) or in modifying the already existing methods (Chen *et al.*, 2007; Ponti *et al.*, 1991).

4.1.1 Determination of a suitable protocol for DNA isolation from mouse liver tissue.

In the initial stages of this work, tissue and cell culture DNA was isolated using Invitrogens chaotropic compound DNAzol combined with high salt. Ct-values from short PCR experiments could often differ by 5-10 numbers, which translates to a difference of 30-1000 times of starting DNA template concentrations. Furthermore, no successful long PCR assays were achieved. The DNA samples were quantified by fluorometry using the Qubit Fluorometer that specifically detects dsDNA. Thus one likely explanation for these large differences in Ct-values was contaminations in the DNA isolates. Salt and protein contamination are known to highly influence PCR based methods (Applied Biosystems2006) and were plausible candidates as contributing factors. Chomczynski (Chomczynski *et al.*, 1997) has previously stated that DNAzol isolated DNA is suitable for any PCR method.

Although when we started isolating DNA using anion-exchange columns from the QIAGEN blood and cell culture kit, both PCR assays showed significantly higher amplification rates per amount of DNA. We conclude that DNA isolated by DNAzol / high salt as not recommendable without further purification for PCR assays, whereas DNA isolated using anion-exchange columns are well suited for PCR assays. This conclusion is supported also by others (Ballinger *et al.*, 1999; Chen *et al.*, 2007; Santos *et al.*, 2006).

4.1.2 Establishing suitable DNA quantification methods for determining template concentrations.

When working with nanogram levels of DNA to be used for quantitative PCR assays, it is highly important to use accurate quantification methods to give correct results. The PCR assays for detecting DNA damage are highly dependent on accurate quantification and also the quality of the DNA template. Studies where accurate knowledge of DNA concentrations are important have consistently used methods based on or related to fluorometric determination, such as the Qubit fluorometer (Ballinger *et al.*, 1999; Chen *et al.*, 2007; Santos *et al.*, 2006).

Fluorometric analysis of DNA concentrations was in this thesis suggested to have a higher level of accuracy and consistency when being compared to spectrophotometrical determination (Table 1). Coincidently, a similar test was done by Invitrogen in early 2011. They report strikingly similar results as our observations (Appendix A). A technical aspect of the experiment that presented a problem was trusting the DNA concentration of the standards. Reasoning concluded that consistency among the sample measurements was a more important issue, therefore this problem was overlooked.

Fluorometric analysis is based on fluorescent dyes, such as Picogreen, that selectively bind dsDNA. When bound to dsDNA, fluorescence enhancement of the dye is exceptionally high. Since the background fluorescence of these dyes is virtually zero, and the dye is only selective to dsDNA. Sample contaminations such as single stranded DNA, proteins and phenols will have no impact on the final fluorescence that is read by the instrument. We have yet to come across any published work discussing problems and disadvantages concerning the fluorometric based Qubit Fluorometer.

Spectrophotometrical determination of DNA is highly influenced by contaminants that absorb light between 260-280 nm (phenols, proteins and single stranded DNA), where dsDNA is also detected. DNA samples measured on the Nanodrop 1000, an instrument based solely on spectrophotometry, is said to contain little to no phenol or protein contamination when the absorbance ratio of 260 / 280 is within 1.8-2.0, and therefore aids the user in determining the purity of their DNA sample. This information may be misleading though, as reports have shown that as much as 60 % protein contamination can still be present when this ratio is observed (Glasel 1995). This restricts the potential for accurate determination of DNA concentrations when using spectrophotometry.

The costs of the Qubit fluorometer is roughly 10 % that of the Nanodrop 1000 (Fisher Scientific 2011), although the Nanodrop 1000 has a larger range of molecules capable of being measured. Using the Qubit fluorometer has higher running costs than the Nanodrop 1000 since the fluorometric dye, buffers and standards have to purchased. When comparing user friendliness, the Nanodrop 1000 was promoted as highly dependable for detecting DNA concentrations from between 2-3700 ng / µl (without dilution) (Nano Drop 2011), although we failed to observe this dependability at the lower regions of this range (Table 1). This could however be due to other components of our DNA samples than DNA itself, such as salts and proteins. Hoever, the large range of the Nanodrop 1000 makes it easier to work with than the Qubit Fluorometer, which can only measure DNA concentrations within two ranges, one between 0.2-100 ng / µl and the other between 2-1000 ng / µl (Invitrogen 2011). Having to constantly switch between each range is time consuming, as they also contain their own set of buffers and calibration standards have to be established for each of them for every run.

We concluded that fluorometric analysis using the Qubit Fluorometer was chosen as the most appropriate method for quantification of DNA concentrations, due to the observation that measurements within the same samples were highly consistent (Table 1). This alone would allow us to confidently assess DNA template concentrations in the coming experiments. The spectrophotometric analysis by using Nanodrop 1000 was however useful for rapid assessments of contaminations in each DNA sample.

4.1.3 Optimizing the short mt-PCR assay.

We were concerned that the 6 min denaturation stage of the short mt-PCR assay was too short for efficient separation of the genomic template, so we opted to test a prolonged denaturation time of 10 min (figure 1). Criteria that would be considered important were low standard deviations between samples and differences in mean Ct-values between the denaturation times (6 and 10 min). Although a marginal lower Ct-value (indicating that product formation is more effective) was observed with the 10 min denaturation, 6 min denaturation time was considered sufficient. Opting to permanently increase the denaturation time to 10 min had to show a larger impact on the Ct-values for us to initiate a change, as instances of template degradation due to long initial denaturation times has been reported (Gustafson *et al.*, 1993). Additionally, there was no observable difference in the standard deviations between samples at the different denaturation times (table 2).

An assumption of the short mt-PCR assay is that due to the very small size of the amplicon, there is a very small likelihood that DNA adducts will form within the 117 bp region of the mitochondrial genome. This was confirmed due to the efficiency of the PCR assay at all dilutions of 1:10 and below (figure 3). However, the linearity of the 3 ng / µl B(a)P (figure 2 C) is affected at the 1:1 dilution. We conclude that the lack of linearity is most likely explained by inhibiting components in the DNA solution, pipetting errors or other systematic mistakes, as the chance of introducing a B(a)P "hit" to so many templates in the 117 bp region in every replicate is extremely unlikely.

These efficiency experiments suggested that an appropriate starting concentration of DNA was at 1:10 (of either 3 or 5 ng / µl), which was therefore chosen onwards. The findings also support that the 117 bp fragment is small enough to not be affected by introduction of DNA adducts.

4.1.4 Optimizing the long mt-PCR assay.

The optimization experiments resulted in the decision to run the long mt-PCR assay using 64 ºC as annealing temperature, in the presence of DNAse-free BSA and DNA concentrations of 5 ng / µl diluted 1:10. These alterations increased the amplification of the 10 kb mitochondrial

fragment compared with other samples with different variables (figure 4). The addition of BSA was suggested by Santos (2006), and is often used in PCR experiments to increase yields as it can counteract substances that inhibit the enzyme activity of the DNA polymerase (Akane *et al.*, 1993; Rossen *et al.*, 1992). It is still advised to check amplification rates with or without BSA in future experiments, as there is instances where the addition of BSA has no implication on product formation (Kreader 1996).

4.2 Establishment of the mitochondrial DNA damage assay (MDDA) in cultivated cells or frozen tissues from mice.

Following the initial optimization of the DNA isolation and quantification protocols, along with the improvements to both the short- and long-mt PCR assays, studies on cultured cells and tissue samples were initiated.

4.2.1 MDDA on DNA from cells exposed to H_2O_2 *in vitro*.

Hydrogen peroxide is produced at low levels by the electron transport chain in mitochondria (Turrens and Boveris 1980), and is known for its ability to generate an array of oxidized DNA lesions (Termini2000).

In our experiments, cultured cells exposed to high levels of H_2O_2 showed a significant loss of mitochondrial template at each exposure (figure 6A) and a reduced level of relative amplification of the large fragment (figure 6B) indicative of DNA damage in the mitochondrial template. The loss of mitochondrial templates were amplified with increasing exposure levels, and statistical significant differences were observed.

When adjusting the long PCR amplifications for the loss of mitochondrial templates, cells exposed to increasing concentrations showed higher amplification values. This may be explained by the very high exposure levels used, probably leading to selection of cells due to mere cell death. Cytotoxicity was however not assessed in these experiments.

The lesions per 10 kb ratio and long fragment amplification rates agrees with previous work, although only at the 100 μM exposure level, as higher dosage than 200 μM have not been reported (Ballinger *et al.*, 1999; Santos *et al.*, 2006). The reasoning for exposure to such high doses was to ensure that the MDDA had ample damage levels to detect, as we were still in the testing stages and were unsure of its sensitivity.

We confirm that mt-DNA is highly susceptible to DNA damage induced by H_2O_2, and that concentrations between 100- 200 μM are more than sufficient for detecting this. More important, the established MDDA could be used for cells in culture, and able to detect DNA damage formed by exposure to genotoxic chemicals.

4.2.2 Frozen liver tissue from mice exposed to B(a)P *in vivo*.

DNA from frozen liver tissue was isolated from three liver samples (unexposed wild-type, B(a)P-exposed wild-type and unexposed OGG1 knockout), and tested to see if the MDDA was capable of detecting DNA damage induced *in vivo* by sub-lethal doses of B(a)P. We hypothesized that the B(a)P exposed wild-type would show the highest detectable damage, followed by the unexposed knockout and at last the unexposed wild-type. However, we are aware of the limitations involved when working with frozen DNA, as the basal DNA damage is markedly increased when freezing biological samples (Fairbairn *et al.*, 1994).

Our results indicate that the B(a)P exposed wild-type had the highest level of mitochondrial template loss, and that this value was significantly different from the unexposed sample (figure 5A), followed by the unexposed wild-type. When adjusting for the loss of mitochondria, the unexposed wild-type has the lowest level of mitochondrial DNA damage, followed by unexposed knockout and B(a)P exposed wild type, as hypothesized. The changes were not statistically significantly different from each other, probably due to the low numbers of samples analysed.

Our original hypothesis of being able to detect DNA damage in frozen tissue still stands, due with the observation that the B(a)P exposed wild-type showed both the largest loss of mitochondrial template and the lowest amplification of the large fragment. The sensitivity of the MDDA in frozen tissue samples is lower than when using freshly harvested tissues,

probably due to spuriously induced DNA lesion during freezing. Comparable results of lesion formation and mitochondrial template loss were qualitatively comparable to results with fresh liver tissue experiments (figure 3 and table 3).

Unexpectedly, the unexposed wild-type had lower levels of mitochondrial template than the unexposed knockout. No sound conclusion onto possible differences between genotypes can be made based on such few biological samples. The difference observed could be caused by DNA damage induced by freezing and thawing of the liver tissue. We therefore conclude that DNA damage induced by B(a)P is detectable compared to unexposed controls, even in frozen tissue. However, the exact level of damage attributed to B(a)P exposure is unclear in frozen tissue and future experiments should preferably be done on fresh tissue to circumvent the challenge of freezing-induced DNA damage and to increase the sensitivity of the assay

4.3 Detection of mitochondrial DNA damage in mice after *in vivo* exposure to B(a)P.

Metabolites of B(a)P, most notably BPDE, bind covalently via its epoxide ring to the dinucleotides deoxyadenosine and deoxyguanosine Our hypothesis was that these DNA alterations may be responsible for reducing mitochondrial template efficiency by haltering the progression of DNA polymerases during DNA synthesis.

The established MDDA, having been successful in its verification stages, was now applied to fresh tissue.

4.3.1 DNA damage in somatic cells: liver.

Our results from four separate *in vivo* experiments demonstrate that liver cells from B(a)P exposed mice exhibit a significant loss of mitochondria genome molecules (figure 5A,C,E and G) and lower amplification rates of the 10 kb mitochondria fragment when compared to the concurrent control (fig 5B,D,F and H). The loss of mitochondrial template is comparable to that observed in frozen tissue. A higher mean rate of DNA lesions per 10 kb is measured in fresh tissue due to exposure-related changes in long fragment amplifications.

B(a)P adducts to DNA has been demonstrated previously directly with other techniques such as high performance liquid chromatography or by using indirect biomarkers (Mensing *et al.*, 2005; Zenzes *et al.*, 1999). There is to our knowledge no successful studies done where PCR based methods are used to detect DNA adducts formed by B(a)P or its metabolites. Attempts have been made, but small amplification targets (< 200 bp) seemed to have missed the B(a)P adducts that would have been randomly distributed along the genome (Denissenko *et al.*, 1994).

B(a)P exposure has been shown to induce chromosomal deletions, single base insertions and deletion mutations (Mizusawa *et al.*, 1981; Zhu *et al.*, 2008). Increasing the number of mutations present in important regions of the mitochondrial genome, for instance those involved in replication and transcription (D-loop) has been reported to lead to a decline in mt-DNA copy numbers (Hebert *et al.*, 2010). This is in line with our observations of loss of mitochondrial template (fig. 7 and 11). It must be stated that this example alone is not sufficient to explain the rate of mitochondrial template loss we observed.

Loss of mitochondrial template has been suggested to arise due to the effects of ageing (Barazzoni *et al.*, 2000; Welle *et al.*, 2003), and hypothesis with regards to ageing is the progressively accumulation of DNA lesions. In line with this the B(a)P-exposed mice in our experiments have experienced large increases in oxidized DNA damage, which can be compared with the amount of oxidative damage that accumulates over a life time. Barazzoni reports a decline of 50 % of mitochondrial template when comparing 6 month old mice (young adults) to 27 month old mice (near death). Our observations of a ~ 20 % reduction of mitochondrial template due to a single exposure is therefore less than the long term effects believed to be due to oxidative damage during the cellular ageing processes, although equivalent to 5 min *in vitro* exposure of 200 μM H_2O_2 (Santos *et al.*, 2006).

Many disagree with the idea that oxidative damage accumulated over life induces loss of mitochondrial template and believe that the differences observed between the different ages are minimal (Frahm *et al.*, 2005; Miller *et al.*, 2003). Others have proposed somewhat the opposite, that an increase in mitochondrial template is observed the older an animal gets (Masuyama *et al.*, 2005). When viewing these arguments, two reasons for explaining this spread of results are probable. First, the method for quantifying mt-DNA influences the results and makes it hard to compare two independent studies using different quantitative

tools. Second, and perhaps the most important, is that the conflicting results may be due to tissue specific differences, as the observations reported are generated in various tissues.

Based on our observations, our hypothesis that B(a)P exposure *in vivo* is capable of inducing DNA adducts- and reducing the template in mitochondria is supported – at least in liver tissue.

4.3.2 DNA damage in male germ cells: sperm.

Our main aim for this Msc-thesis was to establish a simple method for measuring DNA integrity in sperm. However, due to the large work involved with optimizing the methods involved in the MDDA, and the extensive testing and verification of this procedure, we have not been successful in obtaining viable data. However, a novel method for isolating sperm mitochondrial DNA was established and adequate amounts of sperm mt-DNA were isolated using this method. Moreover unique fragments (117 bp and 10 kb) both with the short and long mt-PCR assays were successfully amplified (figure 12 and 13).

4.4 Effects of paternal exposure to B(a)P or and GA on fertilization and early embryo development.

Due to the reports of decreasing fertility rates and sperm quality of males (Auger *et al.*, 1995; Carlsen *et al.*, 1992; Hull *et al.*, 1985), the necessity to explain these findings is escalating in the scientific environment. *In vitro* fertilization is therefore in strong demand, and has also the potential to become an important tool in detecting the causation of the previously mentioned problems.

We aimed at elucidating if high single exposures of B(a)P or GA to males are involved in decreasing fertilization rates or disturbing early embryo development. This set of experiments are a part of a larger project, investigating the impact of sperm DNA lesions on fertilization, early embryo development, and miRNA and mRNA expression during early embryo development following fertilization with sperm from exposed mice.

4.4.1 Counting embryos at different developmental stages.

Previous work done by our lab has shown DNA lesions induced in late spermatids persist in sperm (Olsen *et al.*, 2010), The consequences of paternally transferred DNA lesions are however still unclear. With respect to GA exposure, heritable genomic changes and dominant lethal effects are most evident after exposure to the later stages of spermatogenesis and spermiogenesis (Shelby *et al.*, 1986; Shelby 1996) and it is likely that these effects are associated with persistent DNA adducts present in the fertilizing sperm.

We report a significant decrease in fertilization rates from sperm of mice that have been exposed to either GA or B(a)P (fig. 14 and 16). This decrease in fertilization is in line with a gene expression project also conducted by our lab, the results of which will be published shortly. In brief, results from gene expression experiments suggest that developmental genes are down regulated in 1- and 2-cell embryos fertilized with GA exposed sperm. Our reported decreases in fertilization are consistent with the exisiting literature (Marchetti *et al.*, 1997; Shelby *et al.*, 1986).

After fertilization the progression to the next stages of early embryo development seem to be rather similar between the control and the exposed samples (fig.17). This is also noticed in the gene expression project, where an up-regulation of these developmental genes occurs at the 8-cell stage.

Trans-generational effects of DNA adducts have been reported previously. Smoking may serve as a classical example of xenobiotic exposure with potential transgenerational health effects. Sperm from smoking males typically exhibits higher levels of DNA fragmentation and base adduct formation (Fraga *et al.*, 1996). Sperm from smoking males still retain their capacity to fertilize the oocyte, but it has been reported that the offspring of smoking males experience higher incidence of childhood cancer (Ji *et al.*, 1997).

The inter-experimental difference in fertilization rates between GA and B(a)P experiments is rather high (fig. 14. and 16). This is most likely due to increased efficiency and practical skills that were developed over the two years of this thesis. The handling, accuracy and consistency of the personell involved in these experiments increased during the course of this study. The

improved handling reduced the influence of factors such as temperature and pH that can greatly alter fertilization rates.

With respect to technical details in these experiments, the exposure level of GA and B(a)P is much higher than would be expected in a natural environment but lower than those used for studying dominant lethality (Generoso *et al.*, 1982; Marchetti *et al.*, 1997).

4.5 Conclusions

To reach our vision of establishing a method to detect sperm DNA integrity and understand its consequences for fertilization and early embryo development, we constructed a strategy for detecting DNA lesions in sperm. The chosen method was based on the amplification of a small PCR fragment for assessing mitochondria template concentrations, and a long PCR fragment for the detection of DNA damage. The mitochondrial genome was chosen as proxy for nuclear DNA, due to its higher susceptibility for induction of DNA damage.

To accomplish this we had to successfully isolate mt-DNA from sperm, along with determining accurate DNA quantification methods. A novel simple and rapid method for isolation of mitochondrial sperm DNA was established, based on use of Triton-X, protein digestion and removal of excess biological material. The current method warrants further optimization. In somatic tissue, liver, we conclude that DNA isolation is best achieved by using the anion-exchange column based methods such as those offered from QIAGEN. Fluorometric quantification of DNA demonstrated a high level of consistency (table 1), and was opted as suitable for determining nanogram levels of DNA.

Modifications to the short mt-PCR method included establishing appropriate denaturation times (fig. 1) and determining efficiency of the short mt-PCR assay (fig. 2 and 3). The long PCR assay was optimized with respect to annealing time, addition of BSA and identification of suitable template concentrations (fig. 4)

Due to these optimizations the mitochondrial DNA damage assay (MDDA) was established. By using this new tool, we verified the working procedure of the MDDA in both liver cells exposed *in vitro* to H_2O_2 (fig 6A and B), and in frozen liver cells from mice exposed *in vivo* to B(a)P (fig 7A and B).

Fresh liver tissue from B(a)P exposed mice were tested with the MDDA, showing a significant reduction of mitochondria template (fig 11A,C,E and G). The long PCR assay also managed to detect a difference of approximately 20 % in amplification products between B(a)P exposed and control mice showing that B(a)P-exposed mice exhibit higher levels of DNA damage, even when adjusting for the initial loss of mitochondrial template (fig.11B,D,F and H).

We were only partially successful when considering sperm cells, due to time constraints. The novel method for extracting non contaminated DNA from sperm cells is established, but not yet fully optimized. No valid data on exposure vs. amplification or loss of mitochondria template (fig. 12 and 13) was therefore obtained within the time-frame of this MSc-thesis.

By using in vitro fertilization techniques we managed to observe a significant difference in fertilization rates for B(a)P and GA exposed embryos (fig.14 and 16), whereas early embryonal development as assessed by progression of development was not observed (fig 17). By this we conclude fertilization is affected by preconceptional paternal exposure to Benzo(a)pyrene and Glycidamide.

4.6 Future work

MDDA for detecting DNA damage is established for liver tissue and can be utilised to understand effects mediated via mitochondrial DNA damage or using the MDDA as a sensitive proxy for DNA lesions introduced into nuclear. The study of effects of more relevant exposure scenarios of B(a)P or GA, chronic low doses is useful to understand the impact of such exposures on humans

The MDDA method in sperm has great potential as method to include in andrology or infertility clinics to evaluate DNA integrity of sperm samples, but clearly warrants extensive optimisation first. The novel method for extracting DNA from sperm cells requires more attention and should be further optimized. More extensive experimenting with different concentrations of Triton X-100 would be a wise decision, as the effectiveness of the PCR

methods are dependent on stable template and the lowest levels of contamination as possible. Identifying the most appropriate conditions for protein digestion could also contribute to less contamination and lead to more robust PCR assays giving consistent amplifications.

The method could be used on GA exposed animals, to further document the effects and validate the results observed in our *in vitro* fertilization experiments to GA.

Counting fertilization rates can be used to detect the negative effects on fertility due to paternal exposure to environmental chemicals, especially when combined with gene expression analysis.

Understanding how environmental chemicals affect fertility will allow industrialized countries, where these chemicals are most abundant, to take the necessary precautions to secure the safe continuation of teh human species as well as the quality of life of its citizens

Reference List

Ahmadi, A., and Ng, S. C. (1999). Fertilizing ability of DNA-damaged spermatozoa. *J Exp Zool.* **284,** 696-704.

Akane, A., Shiono, H., Matsubara, K., Nakamura, H., Hasegawa, M., and Kagawa, M. (1993). Purification of forensic specimens for the polymerase chain reaction (PCR) analysis. *J Forensic Sci* **38,** 691-701.

Alberts, Johnson, Lewis, Raff, Roberts, and Walter (2002). Molecular Biology of the Cell, p. Chapter 20-Chapter 21.

Alexandrov, K., Rojas, M., and Satarug, S. (2010). The critical DNA damage by benzo(a)pyrene in lung tissues of smokers and approaches to preventing its formation. *Toxicol Lett.* **198,** 63-68.

Allen, D. C. C. Spectrophotometry http://www.nist.gov/pml/div685/grp03/spectrophotometry.cfm. 5-10-2010.
Ref Type: Online Source

Anderson, S., Bankier, A. T., Barrell, B. G., de Bruijn, M. H., Coulson, A. R., Drouin, J., Eperon, I. C., Nierlich, D. P., Roe, B. A., Sanger, F., Schreier, P. H., Smith, A. J., Staden, R., and Young, I. G. (1981). Sequence and organization of the human mitochondrial genome. *Nature* **290,** 457-465.

Anson, R. M., Hudson, E., and Bohr, V. A. (2000). Mitochondrial endogenous oxidative damage has been overestimated. *FASEB J* **14,** 355-360.

Applied Biosystems. GeneAmp XL PCR kit. 2006.
Ref Type: Pamphlet

Applied Biosystems. Absolute Quantification Getting Started Guide http://www3.appliedbiosystems.com/cms/groups/mcb_support/documents/generaldocuments/cms_042679.pdf. 2011.
Ref Type: Online Source

Auger, J., Kunstmann, J. M., Czyglik, F., and Jouannet, P. (1995). Decline in semen quality among fertile men in Paris during the past 20 years. *N Engl J Med* **332,** 281-285.

Avery.O.T., Macleod, C. M., and McCARTY, M. (1944). Studies on the chemical nature of the substance inducing transformation of pneumococcal types: Induction of transformation by a desoxyribonucleic acid fraction isolated from pneumococcus type III. *J Exp Med* **79,** 137-158.

Ayala-Torres, S., Chen, Y., Svoboda, T., Rosenblatt, J., and Van, H. B. (2000). Analysis of gene-specific DNA damage and repair using quantitative polymerase chain reaction. *Methods* **22,** 135-147.

Ballinger, S. W., Van, H. B., Jin, G. F., Conklin, C. A., and Godley, B. F. (1999). Hydrogen peroxide causes significant mitochondrial DNA damage in human RPE cells. *Exp Eye Res* **68,** 765-772.

Bansal, A. K., and Bilaspuri, G. S. (2010). Impacts of oxidative stress and antioxidants on semen functions. *Vet. Med Int* **2010**.

Barazzoni, R., Short, K. R., and Nair, K. S. (2000). Effects of aging on mitochondrial DNA copy number and cytochrome c oxidase gene expression in rat skeletal muscle, liver, and heart. *J Biol Chem* **275,** 3343-3347.

Birch, D. E. (1996). Simplified hot start PCR. *Nature* **381,** 445-446.

Bjorge, C., Brunborg, G., Wiger, R., Holme, J. A., Scholz, T., Dybing, E., and Soderlund, E. J. (1996). A comparative study of chemically induced DNA damage in isolated human and rat testicular cells. *Reprod. Toxicol* **10,** 509-519.

Bohr, V. A. (2002). Repair of oxidative DNA damage in nuclear and mitochondrial DNA, and some changes with aging in mammalian cells. *Free Radic. Biol Med* **32,** 804-812.

Briede, J. J., Godschalk, R. W., Emans, M. T., de Kok, T. M., Van, A. E., Van, M. J., van Schooten, F. J., and Kleinjans, J. C. (2004a). In vitro and in vivo studies on oxygen free radical and DNA adduct formation in rat lung and liver during benzo[a]pyrene metabolism. *Free Radic. Res* **38,** 995-1002.

Briede, J. J., Godschalk, R. W., Emans, M. T., de Kok, T. M., Van, A. E., Van, M. J., van Schooten, F. J., and Kleinjans, J. C. (2004b). In vitro and in vivo studies on oxygen free radical and DNA adduct formation in rat lung and liver during benzo[a]pyrene metabolism. *Free Radic. Res* **38,** 995-1002.

Brison, D. R., and Schultz, R. M. (1997). Apoptosis during mouse blastocyst formation: evidence for a role for survival factors including transforming growth factor alpha. *Biol Reprod.* **56,** 1088-1096.

Brookes, P., and Lawley, P. D. (1964). Evidence for the binding of polynuclear aromatic hydrocarbons to the nucleic acids of mouse skin: Relation between carcinogenic power of hydrocarbons and their binding to deoxyribonucleic acid. *Nature* **202,** 781-784.

Brown, T. A. (2006). Genomes 3.

Calleman, C. J., Bergmark, E., and Costa, L. G. (1990). Acrylamide is metabolized to glycidamide in the rat: evidence from hemoglobin adduct formation. *Chem Res Toxicol* **3,** 406-412.

Carlsen, E., Giwercman, A., Keiding, N., and Skakkebaek, N. E. (1992). Evidence for decreasing quality of semen during past 50 years. *BMJ* **305,** 609-613.

Chan, D. C. (2006). Mitochondria: dynamic organelles in disease, aging, and development. *Cell* **125,** 1241-1252.

Chen, J., Kadlubar, F. F., and Chen, J. Z. (2007). DNA supercoiling suppresses real-time PCR: a new approach to the quantification of mitochondrial DNA damage and repair. *Nucleic Acids Res* **35,** 1377-1388.

Chien, A., Edgar, D. B., and Trela, J. M. (1976). Deoxyribonucleic acid polymerase from the extreme thermophile Thermus aquaticus. *J Bacteriol.* **127,** 1550-1557.

Chomczynski, P., Mackey, K., Drews, R., and Wilfinger, W. (1997). DNAzol: a reagent for the rapid isolation of genomic DNA. *Biotechniques* **22,** 550-553.

Curtis D.Klaassen (2008). Casarett & Doull's Toxicology, The Basic Science of Poisons..

Dahm, R. (2010). From discovering to understanding. Friedrich Miescher's attempts to uncover the function of DNA. *EMBO Rep* **11,** 153-160.

Denissenko, M. F., Venkatachalam, S., Yamasaki, E. F., and Wani, A. A. (1994). Assessment of DNA damage and repair in specific genomic regions by quantitative immuno-coupled PCR. *Nucleic Acids Res* **22,** 2351-2359.

Fairbairn, D. W., Reyes, W. A., Van, G. R., and O'Neill, K. L. (1994). Laser scanning microscopic analysis of DNA damage in frozen tissues. *Cancer Lett.* **76,** 127-132.

Fertaid. History of In Vitro Fertilization http://www.fertaid.com. 2011.
Ref Type: Online Source

Fisher Scientific. Fisher Scientific. 2011.
Ref Type: Online Source

Fraga, C. G., Motchnik, P. A., Wyrobek, A. J., Rempel, D. M., and Ames, B. N. (1996). Smoking and low antioxidant levels increase oxidative damage to sperm DNA. *Mutat. Res* **351,** 199-203.

Frahm, T., Mohamed, S. A., Bruse, P., Gemund, C., Oehmichen, M., and Meissner, C. (2005). Lack of age-related increase of mitochondrial DNA amount in brain, skeletal muscle and human heart. *Mech. Ageing Dev* **126,** 1192-1200.

Freeman, W. M., Walker, S. J., and Vrana, K. E. (1999). Quantitative RT-PCR: pitfalls and potential. *Biotechniques* **26,** 112-115.

Friedberg, Walker, Siede, Wood, Schultz, and Ellenberger (2006). DNA Repair and Mutagenesis, pp. 9-57.

Gao, D., Wei, C., Chen, L., Huang, J., Yang, S., and Diehl, A. M. (2004). Oxidative DNA damage and DNA repair enzyme expression are inversely related in murine models of fatty liver disease. *Am J Physiol Gastrointest. Liver Physiol* **287,** G1070-G1077.

Gelboin, H. V. (1980). Benzo[alpha]pyrene metabolism, activation and carcinogenesis: role and regulation of mixed-function oxidases and related enzymes. *Physiol Rev* **60,** 1107-1166.

Generoso, W. M., Cain, K. T., Hellwig, C. S., and Cacheiro, N. L. (1982). Lack of association between induction of dominant-lethal mutations and induction of heritable translocations with benzo[a]pyrene in postmeiotic germ cells of male mice. *Mutat. Res* **94,** 155-163.

Generoso, W. M., Sega, G. A., Lockhart, A. M., Hughes, L. A., Cain, K. T., Cacheiro, N. L., and Shelby, M. D. (1996). Dominant lethal mutations, heritable translocations, and unscheduled DNA synthesis induced in male mouse germ cells by glycidamide, a metabolite of acrylamide. *Mutat. Res* **371,** 175-183.

Glasel, J. A. (1995). Validity of nucleic acid purities monitored by 260nm/280nm absorbance ratios. *Biotechniques* **18,** 62-63.

Griveau, J. F., and Le, L. D. (1997). Reactive oxygen species and human spermatozoa: physiology and pathology. *Int J Androl* **20,** 61-69.

Gustafson, C. E., Alm, R. A., and Trust, T. J. (1993). Effect of heat denaturation of target DNA on the PCR amplification. *Gene* **123,** 241-244.

Harrouk, W., Codrington, A., Vinson, R., Robaire, B., and Hales, B. F. (2000). Paternal exposure to cyclophosphamide induces DNA damage and alters the expression of DNA repair genes in the rat preimplantation embryo. *Mutat. Res* **461,** 229-241.

Hattemer-Frey, H. A., and Travis, C. C. (1991). Benzo-a-pyrene: environmental partitioning and human exposure. *Toxicol Ind. Health* **7,** 141-157.

Hayden, M. J., Nguyen, T. M., Waterman, A., and Chalmers, K. J. (2008). Multiplex-ready PCR: a new method for multiplexed SSR and SNP genotyping. *BMC Genomics* **9,** 80.

Hebert, S. L., Lanza, I. R., and Nair, K. S. (2010). Mitochondrial DNA alterations and reduced mitochondrial function in aging. *Mech. Ageing Dev* **131,** 451-462.

Helbock, H. J., Beckman, K. B., Shigenaga, M. K., Walter, P. B., Woodall, A. A., Yeo, H. C., and Ames, B. N. (1998). DNA oxidation matters: the HPLC-electrochemical detection assay of 8-oxo-deoxyguanosine and 8-oxo-guanine. *Proc Natl. Acad. Sci U S A* **95,** 288-293.

Henze, K., and Martin, W. (2003). Evolutionary biology: essence of mitochondria. *Nature* **426,** 127-128.

Higuchi, R., Fockler, C., Dollinger, G., and Watson, R. (1993). Kinetic PCR analysis: real-time monitoring of DNA amplification reactions. *Biotechnology (N Y)* **11,** 1026-1030.

Honig, S. C., Lipshultz, L. I., and Jarow, J. (1994). Significant medical pathology uncovered by a comprehensive male infertility evaluation. *Fertil. Steril.* **62,** 1028-1034.

Hull, M. G., Glazener, C. M., Kelly, N. J., Conway, D. I., Foster, P. A., Hinton, R. A., Coulson, C., Lambert, P. A., Watt, E. M., and Desai, K. M. (1985). Population study of causes, treatment, and outcome of infertility. *Br Med J (Clin Res Ed)* **291,** 1693-1697.

Hwang, K., Walters, R. C., and Lipshultz, L. I. (2011). Contemporary concepts in the evaluation and management of male infertility. *Nat Rev Urol.*

IARC. IARC http://www.iarc.fr/. 2011.
Ref Type: Online Source

Invitrogen. Qubit Manual http://www.invitrogen.com/etc/medialib/en/filelibrary/pdf.Par.32407.File.dat/mp32857.pdf . 2011.
Ref Type: Online Source

Ji, B. T., Shu, X. O., Linet, M. S., Zheng, W., Wacholder, S., Gao, Y. T., Ying, D. M., and Jin, F. (1997). Paternal cigarette smoking and the risk of childhood cancer among offspring of nonsmoking mothers. *J Natl. Cancer Inst.* **89,** 238-244.

Kalinowski, D. P., Illenye, S., and Van, H. B. (1992). Analysis of DNA damage and repair in murine leukemia L1210 cells using a quantitative polymerase chain reaction assay. *Nucleic Acids Res* **20,** 3485-3494.

Kim, J. H., Stansbury, K. H., Walker, N. J., Trush, M. A., Strickland, P. T., and Sutter, T. R. (1998). Metabolism of benzo[a]pyrene and benzo[a]pyrene-7,8-diol by human cytochrome P450 1B1. *Carcinogenesis* **19,** 1847-1853.

Kreader, C. A. (1996). Relief of amplification inhibition in PCR with bovine serum albumin or T4 gene 32 protein. *Appl Environ Microbiol* **62,** 1102-1106.

Larsen, E., Kwon, K., Coin, F., Egly, J. M., and Klungland, A. (2004). Transcription activities at 8-oxoG lesions in DNA. *DNA Repair (Amst)* **3,** 1457-1468.

Laws, G. M., Skopek, T. R., Reddy, M. V., Storer, R. D., and Glaab, W. E. (2001). Detection of DNA adducts using a quantitative long PCR technique and the fluorogenic 5' nuclease assay (TaqMan). *Mutat. Res* **484,** 3-18.

Leadon, S. A., Stampfer, M. R., and Bartley, J. (1988). Production of oxidative DNA damage during the metabolic activation of benzo[a]pyrene in human mammary epithelial cells correlates with cell killing. *Proc Natl. Acad. Sci U S A* **85,** 4365-4368.

Lindahl, T. (1993). Instability and decay of the primary structure of DNA. *Nature* **362,** 709-715.

Mangal, D., Vudathala, D., Park, J. H., Lee, S. H., Penning, T. M., and Blair, I. A. (2009). Analysis of 7,8-dihydro-8-oxo-2'-deoxyguanosine in cellular DNA during oxidative stress. *Chem Res Toxicol* **22,** 788-797.

Marchetti, F., Lowe, X., Bishop, J., and Wyrobek, A. J. (1997). Induction of chromosomal aberrations in mouse zygotes by acrylamide treatment of male germ cells and their correlation with dominant lethality and heritable translocations. *Environ Mol Mutagen.* **30,** 410-417.

Masuyama, M., Iida, R., Takatsuka, H., Yasuda, T., and Matsuki, T. (2005). Quantitative change in mitochondrial DNA content in various mouse tissues during aging. *Biochim. Biophys. Acta* **1723,** 302-308.

Mattes, W. B. (1990). Lesion selectivity in blockage of lambda exonuclease by DNA damage. *Nucleic Acids Res* **18,** 3723-3730.

Mensing, T., Marczynski, B., Engelhardt, B., Wilhelm, M., Preuss, R., Kappler, M., Angerer, J., Kafferlein, H. U., Scherenberg, M., Seidel, A., and Bruning, T. (2005). DNA adduct formation of benzo[a]pyrene in white blood cells of workers exposed to polycyclic aromatic hydrocarbons. *Int J Hyg. Environ Health* **208,** 173-178.

Miller, F. J., Rosenfeldt, F. L., Zhang, C., Linnane, A. W., and Nagley, P. (2003). Precise determination of mitochondrial DNA copy number in human skeletal and cardiac muscle by a PCR-based assay: lack of change of copy number with age. *Nucleic Acids Res* **31,** e61.

Miller, K. P., and Ramos, K. S. (2001). Impact of cellular metabolism on the biological effects of benzo[a]pyrene and related hydrocarbons. *Drug Metab Rev* **33,** 1-35.

Mizusawa, H., Lee, C. H., Kakefuda, T., McKenney, K., Shimatake, H., and Rosenberg, M. (1981). Base insertion and deletion mutations induced in an Escherichia coli plasmid by benzo[a]pyrene-7,8-dihydrodiol-9,10-epoxide. *Proc Natl. Acad. Sci U S A* **78,** 6817-6820.

Moline, J. M., Golden, A. L., Bar-Chama, N., Smith, E., Rauch, M. E., Chapin, R. E., Perreault, S. D., Schrader, S. M., Suk, W. A., and Landrigan, P. J. (2000). Exposure to hazardous substances and male reproductive health: a research framework. *Environ Health Perspect* **108,** 803-813.

Mottram, D. S., Wedzicha, B. L., and Dodson, A. T. (2002). Acrylamide is formed in the Maillard reaction. *Nature* **419,** 448-449.

Mullis, K., Faloona, F., Scharf, S., Saiki, R., Horn, G., and Erlich, H. (1986). Specific enzymatic amplification of DNA in vitro: the polymerase chain reaction. *Cold Spring Harb. Symp. Quant. Biol* **51 Pt 1,** 263-273.

Nano Drop. Nano Drop 1000 user manual http://www.mun.ca/biology/dmarshall/nd-1000-users-manual.pdf. 2011.
Ref Type: Online Source

Ni, Z. Y., Liu, Y. Q., Shen, H. M., Chia, S. E., and Ong, C. N. (1997). Does the increase of 8-hydroxydeoxyguanosine lead to poor sperm quality? *Mutat. Res* **381,** 77-82.

Olsen, A. K., Andreassen, A., Singh, R., Wiger, R., Duale, N., Farmer, P. B., and Brunborg, G. (2010). Environmental exposure of the mouse germ line: DNA adducts in spermatozoa and formation of de novo mutations during spermatogenesis. *PLoS One* **5,** e11349.

Olsen, A. K., Duale, N., Bjoras, M., Larsen, C. T., Wiger, R., Holme, J. A., Seeberg, E. C., and Brunborg, G. (2003). Limited repair of 8-hydroxy-7,8-dihydroguanine residues in human testicular cells. *Nucleic Acids Res* **31,** 1351-1363.

Park, J. H., Mangal, D., Frey, A. J., Harvey, R. G., Blair, I. A., and Penning, T. M. (2009). Aryl hydrocarbon receptor facilitates DNA strand breaks and 8-oxo-2'-deoxyguanosine formation by the aldo-keto reductase product benzo[a]pyrene-7,8-dione. *J Biol Chem* **284,** 29725-29734.

Paulsson, B., Granath, F., Grawe, J., Ehrenberg, L., and Tornqvist, M. (2001). The multiplicative model for cancer risk assessment: applicability to acrylamide. *Carcinogenesis* **22,** 817-819.

Penning, T. M. (2004). Aldo-keto reductases and formation of polycyclic aromatic hydrocarbon o-quinones. *Methods Enzymol.* **378,** 31-67.

Phillips, D. H. (1983). Fifty years of benzo(a)pyrene. *Nature* **303,** 468-472.

Pinto, A. L., and Lippard, S. J. (1985). Sequence-dependent termination of in vitro DNA synthesis by cis- and trans-diamminedichloroplatinum (II). *Proc Natl. Acad. Sci U S A* **82,** 4616-4619.

Ponti, M., Forrow, S. M., Souhami, R. L., D'Incalci, M., and Hartley, J. A. (1991). Measurement of the sequence specificity of covalent DNA modification by antineoplastic agents using Taq DNA polymerase. *Nucleic Acids Res* **19,** 2929-2933.

QIAGEN. QIAGEN Genomic DNA Handbook. 1-1-2001.
Ref Type: Catalog

Richter, C., Park, J. W., and Ames, B. N. (1988). Normal oxidative damage to mitochondrial and nuclear DNA is extensive. *Proc Natl. Acad. Sci U S A* **85,** 6465-6467.

Rodriguez-Zas, S. L., Schellander, K., and Lewin, H. A. (2008). Biological interpretations of transcriptomic profiles in mammalian oocytes and embryos. *Reproduction* **135,** 129-139.

Rossen, L., Norskov, P., Holmstrom, K., and Rasmussen, O. F. (1992). Inhibition of PCR by components of food samples, microbial diagnostic assays and DNA-extraction solutions. *Int J Food Microbiol* **17,** 37-45.

Sanova, S., Balentova, S., Slovinska, L., and Misurova, E. (2005). Effects of preconceptional gamma irradiation on the development of rat brain. *Neurotoxicol. Teratol.* **27,** 145-151.

Santos, J. H., Meyer, J. N., Mandavilli, B. S., and Van, H. B. (2006). Quantitative PCR-based measurement of nuclear and mitochondrial DNA damage and repair in mammalian cells. *Methods Mol Biol* **314,** 183-199.

Sawyer, D. E., Mercer, B. G., Wiklendt, A. M., and Aitken, R. J. (2003). Quantitative analysis of gene-specific DNA damage in human spermatozoa. *Mutat. Res* **529,** 21-34.

Sega, G. A., Generoso, E. E., and Brimer, P. A. (1990). Acrylamide exposure induces a delayed unscheduled DNA synthesis in germ cells of male mice that is correlated with the temporal pattern of adduct formation in testis DNA. *Environ Mol Mutagen.* **16,** 137-142.

Segerback, D., Calleman, C. J., Schroeder, J. L., Costa, L. G., and Faustman, E. M. (1995). Formation of N-7-(2-carbamoyl-2-hydroxyethyl)guanine in DNA of the mouse and the rat following intraperitoneal administration of [14C]acrylamide. *Carcinogenesis* **16,** 1161-1165.

Settels, E., Bernauer, U., Palavinskas, R., Klaffke, H. S., Gundert-Remy, U., and Appel, K. E. (2008). Human CYP2E1 mediates the formation of glycidamide from acrylamide. *Arch Toxicol* **82,** 717-727.

Shelby, M. D. (1996). Selecting chemicals and assays for assessing mammalian germ cell mutagenicity. *Mutat. Res* **352,** 159-167.

Shelby, M. D., Cain, K. T., Hughes, L. A., Braden, P. W., and Generoso, W. M. (1986). Dominant lethal effects of acrylamide in male mice. *Mutat. Res* **173,** 35-40.

Shimada, T., and Fujii-Kuriyama, Y. (2004). Metabolic activation of polycyclic aromatic hydrocarbons to carcinogens by cytochromes P450 1A1 and 1B1. *Cancer Sci* **95,** 1-6.

Sims, P., Grover, P. L., Swaisland, A., Pal, K., and Hewer, A. (1974). Metabolic activation of benzo(a)pyrene proceeds by a diol-epoxide. *Nature* **252,** 326-328.

Solomon, J. J., Fedyk, J., Mukai, F., and Segal, A. (1985). Direct alkylation of 2'-deoxynucleosides and DNA following in vitro reaction with acrylamide. *Cancer Res* **45,** 3465-3470.

Stanton, J. A., Macgregor, A. B., and Green, D. P. (2003). Gene expression in the mouse preimplantation embryo. *Reproduction* **125,** 457-468.

Stemmer, W. P., Crameri, A., Ha, K. D., Brennan, T. M., and Heyneker, H. L. (1995). Single-step assembly of a gene and entire plasmid from large numbers of oligodeoxyribonucleotides. *Gene* **164,** 49-53.

Steptoe, P. C., and Edwards, R. G. (1978). Birth after the reimplantation of a human embryo. *Lancet* **2,** 366.

Tadros, W., and Lipshitz, H. D. (2009). The maternal-to-zygotic transition: a play in two acts. *Development* **136,** 3033-3042.

Tareke, E., Rydberg, P., Karlsson, P., Eriksson, S., and Tornqvist, M. (2002). Analysis of acrylamide, a carcinogen formed in heated foodstuffs. *J Agric Food Chem* **50,** 4998-5006.

Termini, J. (2000). Hydroperoxide-induced DNA damage and mutations. *Mutat. Res* **450,** 107-124.

Turrens, J. F., and Boveris, A. (1980). Generation of superoxide anion by the NADH dehydrogenase of bovine heart mitochondria. *Biochem J* **191,** 421-427.

V.Shelkovsky, S. G. S. I. K. G. M. V. K. L. A. Modeling of recognition sites of nucleic acid bases aaand amide side chains of amino acids. Combination of experimental and theoretical approaches . The European Physical Journal D - Atomic, Molecular, Optical and Plasma Physics Volume 20(Number 3), 421-430. 2002.
Ref Type: Journal (Full)

Van Houten B., Chen, Y., Nicklas, J. A., Rainville, I. R., and O'Neill, J. P. (1998). Development of long PCR techniques to analyze deletion mutations of the human hprt gene. *Mutat. Res* **403,** 171-175.

Wang, J., and Sauer, M. V. (2006). In vitro fertilization (IVF): a review of 3 decades of clinical innovation and technological advancement. *Ther Clin Risk Manag.* **2,** 355-364.

Watson, J. D., and Crick, F. H. (1953). Molecular structure of nucleic acids; a structure for deoxyribose nucleic acid. *Nature* **171,** 737-738.

Welle, S., Bhatt, K., Shah, B., Needler, N., Delehanty, J. M., and Thornton, C. A. (2003). Reduced amount of mitochondrial DNA in aged human muscle. *J Appl Physiol* **94,** 1479-1484.

Wellejus, A., Poulsen, H. E., and Loft, S. (2000). Iron-induced oxidative DNA damage in rat sperm cells in vivo and in vitro. *Free Radic. Res* **32,** 75-83.

Wiesner, R. J., Ruegg, J. C., and Morano, I. (1992). Counting target molecules by exponential polymerase chain reaction: copy number of mitochondrial DNA in rat tissues. *Biochem Biophys. Res Commun.* **183,** 553-559.

Yakes, F. M., and Van, H. B. (1997). Mitochondrial DNA damage is more extensive and persists longer than nuclear DNA damage in human cells following oxidative stress. *Proc Natl. Acad. Sci U S A* **94,** 514-519.

Zenzes, M. T., Bielecki, R., and Reed, T. E. (1999). Detection of benzo(a)pyrene diol epoxide-DNA adducts in sperm of men exposed to cigarette smoke. *Fertil. Steril.* **72,** 330-335.

Zheng, S. J., Tian, H. J., Cao, J., and Gao, Y. Q. (2010). Exposure to di(n-butyl)phthalate and benzo(a)pyrene alters IL-1beta secretion and subset expression of testicular macrophages, resulting in decreased testosterone production in rats. *Toxicol Appl Pharmacol* **248,** 28-37.

Zheng, Y., Cloutier, P., Hunting, D. J., Sanche, L., and Wagner, J. R. (2005). Chemical basis of DNA sugar-phosphate cleavage by low-energy electrons. *J Am Chem Soc* **127,** 16592-16598.

Zhu, Y., Horikawa, Y., Yang, H., Wood, C. G., Habuchi, T., and Wu, X. (2008). BPDE induced lymphocytic chromosome 3p deletions may predict renal cell carcinoma risk. *J Urol.* **179,** 2416-2421.

Appendix A

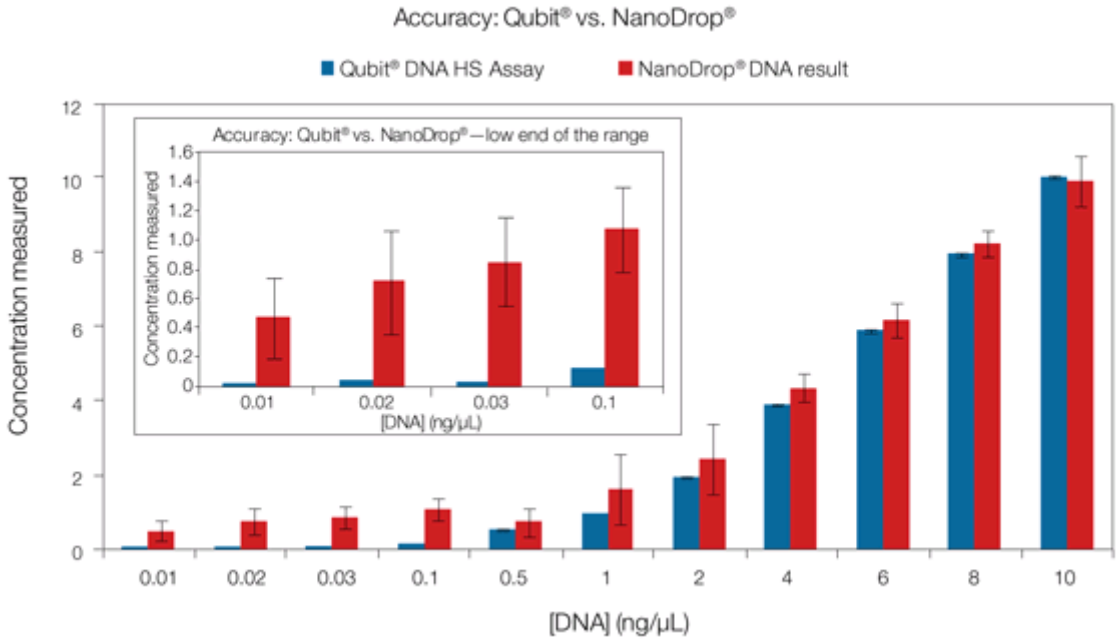

Figure taken from Invitrogens homepage (www.invitrogen.com), displaying comparison between Qubit® 2.0 Fluorometer and NanoDrop® Spectrophotometer.

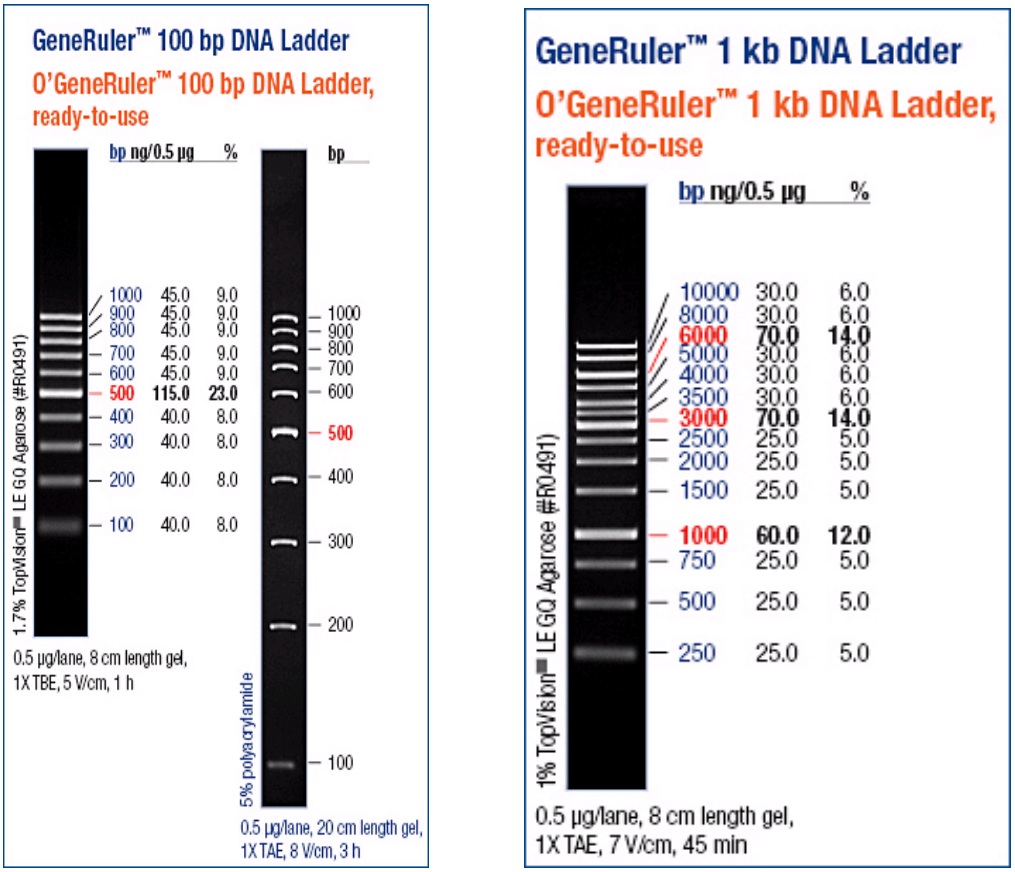

100 bp and 1 kb DNA ladders from Fermentas.

Lane	Content with DNA dilution	Qubit measurement (ng / ul)
1	BSA 1:10	16.6
2	BSA 1:10	2.6
3	BSA 1:100	2.5
4	1:10	16.2
5	1:10	15.1
6	Blank	0
7	Blank	0
8	Blank	0
9	BSA 1:10	17.9
10	BSA 1:10	17.7
11	BSA 1:100	2.5
12	1:10	13.2
13	1:10	13.7
14	Blank	0
15	Blank	0
16	Blank	0
17	BSA 1:10	5.0
18	BSA 1:10	4.4
19	BSA 1:100	1.22
20	1:10	3.3
21	1:10	0.72
22	Blank	0
23	Blank	0
24	Blank	0

Qubit fluorometric results from figure 4. Each lane is as depicted on the gel photo (DNA ladder omitted).

Appendix B

Products and producers:

Product	Producer
25 cm² cell flask, 75 cm² cell flask	Corning
Absolute alcohol prima	Arkus kjemi
Benzo(a)pyrene	Sigma
Bovine serum albumine	Sigma
Cellulyser	TATAA Biocenter
Chelex water/HPLC grade water	Locally produced
CO_2	AGA
Corn oil	Sigma
dH_2O	Bibco
Dounce homogenisator A+B	Fischer
EDTA	Sigma
Eppendorf tubes 1.5 mL	Sigma
Ethidium bromide	Merck
Falcon tubes, 15mL and 60mL	Nunc
FCS	Fischer
GA	Sigma
30 % H_2O_2	Merck
HCG	Sigma
Hepa1c1c7 cell line	Sigma
HTF	Millipore
Isopropanol	ARCUS
KSOM	Millipore
Liquid parafin	Medicult
M2 medium	Sigma
MEM Alpha	GIBCO
MicroAmp 96-well reaction plate	Applied Biosystems
Nanodrop 1000	Nanodrop
NuSieve GTG Low melting Agarose	Cambrex
PBS	Locally produced
PCR 0,5ml Thinwall	AXYGEN
Petri dish	Sigma
PMSG	Intervet
Primers	QIAGEN
Proteinase K	VWR International
QIAGEN Blood and cell kit	QIAGEN
Quant-iT ds DNA BR/HS 500 assays	Invitrogen
Qubit Fluorometer	Invitrogen
RNase A	Sigma
RNase Ti	Fluka
SYBR®Green	Sigma
50X TAE buffer	Locally produced

Triton X	Sigma
Trypsin	Sigma
XL PCR kit	Applied Biosystems
ZipRuler 1 kb and 100 bp	Fermentas